CHEMICAL CHARACTERIZATION OF A hvb COAL

Kwang E. Chung, Larry L. Anderson and Wendell H. Wiser

Department of Mining and Fuels Engineering
University of Utah
Salt Lake City, Utah 84112

Introduction

Numerous physical and chemical means are employed to elucidate the general proper-
ties and nature of coal (1,2,3). Coal has been examined directly as a solid and
indirectly in liquefied form. Nevertheless, our present understanding of coal is
surprisingly limited, preventing us from more efficient utilization of coal for energy
and chemicals.

Ultimate and proximate analyses are routinely performed on coals, but most other
information is general or descriptive. Direct examination of coal by various spectro-
scopic means have resulted in useful, but usually qualitative information. Solvent·
extraction has not been too successful due to poor solubility of coal in known solvents.
Information from coal-derived liquids (CDL) has been related to the structure of coal
only superficially. The complexity and insolubility of coal have defied many ingenious
approaches and modern analytical means as far as the exact chemical nature of coal is
concerned.

Here we report the development of a suitable scheme for characterizing CDL, which
identified and quantified major structural units in a high volatile bituminous coal.
We will describe how this characterization scheme for CDL was formulated, and discuss
the preparation and characterization of three CDL's. Our findings will then be related
to the chemical structure of the particular coal we examined.

Characterization Scheme for CDL

Since a complete analysis of CDL is impractical, if not impossible, due to the
complexity in composition, "characterization" is performed, meaning determination of the
quantitative distribution of compound types and the functional groups present. Although
it is practical to do so, the nature of the characterization work needs to be carefully
examined in terms of purpose, the material to be characterized, and the procedure.

The purpose of characterization in petroleum research has been mainly to obtain
necessary information for further processing of petroleum or its fractions. In coal
research, elucidation of the chemical structure of the CDL precursor (coal) is of much
interest. Improvements in understanding of coal structure is essential in devising a
better characterization scheme for CDL, which in turn will improve our understanding of
coal structure.

Available information on coal and CDL (1-4) was carefully evaluated and incorporated
into a new characterization scheme. Coal was considered as a composite of polymer-like
materials. It may consist of numerous constituents having different types of structural
units and linkages. Accordingly, the liquefaction of coal was assumed as basically a
depolymerization process.

In preparing CDL, the following has been taken into consideration: (1) a CDL should
represent the coal under investigation, (2) the degree of depolymerization needs to be
carefully chosen, and (3) the liquids must be accessible by analytical means possibly
at the molecular level. Based upon these considerations, CDL were prepared in high
conversion processes (with a relatively high degree of depolymerization).

Considering the nature of the depolymerization process, the molecular size was
chosen as a separation criterion for the fractionation of CDL, and vacuum distillation

was employed. For non-distillable CDL solvent extraction was used for separation. Each fraction from the separation was analyzed by elemental analysis, molecular weight determination and NMR spectroscopy. This scheme is different from others(5) previously employed, especially in the preparation of CDL and the methods used for the separations.

Experimental

A hvb coal (Clear Creek, Utah) was liquefied in a dry coiled-tube reactor(6). The coal had 39.1% of volatile matter, and its elemental composition (wt. percent) was: C, 76.1; H, 5.6; N, 1.4; and O, 17.9. Reaction conditions used in the liquefaction process were: T = 500°C; P_{H2} = 1800 psig; catalyst = 5% $ZnCl_2$; and residence time, several seconds. Product yields were: gases, 10%; light liquid, 5%; heavy liquid, 55%; char, 15%; and H_2O, 15% (based on MAF coal).

The heavy liquid had a boiling range from 250°C to more than 500°C, and accounted for more than 70% of the condensed-phase products which included light and heavy liquids, and char. The condensed-phase products were assumed to retain the skeletal structure of coal. This assumption was supported by C^{13} NMR analysis of starting coal and liquid products (7). Thus the heavy liquid was examined further in the subsequent investigation. Paraffinic material in the liquid was removed by solvent extraction. The liquid material remaining after this extraction was designated as HVL-P. HVL-P was distilled at temperatures below 260°C at a pressure of 3 Torr. The distillate was divided into three fractions, Light, Middle and Heavy according to their physical appearance with the non-distillable fraction termed Resid. Light and Middle were fluid at room temperature, but a phase separation appeared between them. Heavy and Resid were solids.

In another preparation of CDL's, the same coal was solubilized by reacting with sodium hydroxide and ethanol at 300°C and 320°C for 100 minutes in an autoclave using a procedure similar to that of Makabe (8). The products were named SP-300 and SP-320, the former being from 300°C runs and the latter being from 320°C runs. Each product was divided into four fractions. Two of them (Fractions I and J in SP 300, and Fractions I' and J' in SP-320) were soluble or floating in a strong basic solution, but precipitated in different fashion upon neutralization. The rest of the products were extracted with pyridine at room temperature to obtain Fractions K and K' (pyridine soluble) and pyridine insoluble portions.

Elemental composition was determined with a Perkin-Elmer Model 240 Analyzer. Oxygen was determined separately. NMR spectra were obtained with an EM-390 spectrometer (Varian). Pyridine-D_5 and $CDCl_3$ were used as solvent. Molecular weights were determined by vapor phase osmoemtry using a Corona Model 117 apparatus (Wescan Instruments, Inc.). The experimental procedure and conditions were carefully chosen to ensure the correct determination of molecular weight (9).

Results and Discussion

Structural parameters of average molecules in the CDL fractions were calculated from the elemental composition, molecular weight and proton NMR spectra. Their definitions and formulae (10) are:

Number of aromatic carbons

$$C_A = C - \frac{1}{2} (H_{2\alpha} + H_\beta) - \frac{1}{3} (H_{3\alpha} + H_\gamma) \tag{1}$$

Fraction of aromatic carbons (=aromaticity)

$$f_A = \frac{C_A}{C} \tag{2}$$

Total number of rings

$$R = \frac{2C - H + 2}{2} - \frac{1}{2} C_A \tag{3}$$

Number of aromatic clusters

$$C_{AP} = H_A + \frac{1}{2} H_{2\alpha} + \frac{1}{3} H_{3\alpha} \qquad (4)$$

$$n = \#cl = \frac{1}{3} (C_{AP} - \frac{1}{2} C_A) \qquad (5)$$

Number of aromatic rings

$$R_A = \frac{1}{4} (C_A - 2n) \qquad (6)$$

Number of naphthenic rings

$$R_N = R - R_A \qquad (7)$$

Values of C and H were from the empirical formula of each fraction. Hydrogen (H) was divided into four types based on NMR spectra: H_A, 5 - 9 ppm; $H_{2\alpha}$, 2.2 - 5 ppm: $H_{3\alpha}$, 2.0-2.2 ppm; H_β , 1.1-2.0 ppm; and H_γ, 0.3-1.1 ppm.

Table 1 summarizes yields from the distillation along with structural parameters of HVL-P fractions. All data are experimental values except for those in parentheses. Values in parentheses were calculated from those of the four fractions. The yields show that Light, Middle and Heavy fractions are a major portion of HVL-P.

Structural parameters change significantly from one fraction to another. For example, number of total rings, R, of HVL-P is 3.2, but it varies from 1.8 to 5.6 in its fractions. The number of total rings decreased by 1.9 from Resid to Heavy, 1.4 from Heavy to Middle, and 0.5 from Middle to Light. The number of aromatic rings, R_A, and molecular weight decreased in a similar fashion.

These differences are so large that the fractions were grouped into three, A, B, and C (Light and Middle, Heavy, and Resid respectively). The number of aromatic clusters (#Cl) reveals that most molecules in the first two groups (A and B) have one aromatic cluster, while about 30% of molecules in C have, on the average, two clusters. Overall, molecules in HVL-P have almost one aromatic cluster, indicating that HVL-P was essentially completely depolymerized.

Structural parameters were used to sketch possible structures of the four fractions. The structures in Fig. 1 contain the appropriate numbers of aromatic rings, aromatic clusters and naphthenic rings. The presence of functional groups or side chains on the structures are qualitative.

If one assumes that the aromatic double bonds were neither produced nor broken during the liquefaction process (in the production of HVL-P), the components in Group C were not converted to substantially smaller molecules (like A or B). Also Group B molecules were not converted to Group A. This non-convertibility indicates that the three groups were produced from three different structural units of the feed coal.

The assumption was drawn from the following consideration: (1) the liquefaction conditions were unfavorable for hydrogenation or dehydrogenation of aromatic structure in coal: most notably the residence time was too short, and (2) the large differences in molecular size among the three groups would have not resulted from the conversion of a large component group to a smaller one. Examination of the solubilization products, SP-300 and SP-320, provides further supporting information for this assumption as well as other interesting features of coal structure.

Table 2 contains yields and structural parameters of the solubilization products. As expected from the experimental conditions, the yields and molecular size of the products are substantially larger than those of HVL-P. Yet comparison of the structural parameters of HVL-P and SP-300 reveals a remarkable resemblance in an important structural feature: the average aromatic cluster sizes, $R_A/\#cl$, are the same, 2.2, in both products. This agreement can be related to approximate size of the average aromatic cluster in coal.

Considering that 15% of the char yield and 5% of the light liquid yield in pro-
ducing HVL-P, the average aromatic cluster size of the condensed-phase products
(HVL-P, light liquid and char), which are supposed to retain the skeletal structure of
coal, is expected to be larger than 2.2. On the other hand, SP-300 represents more
than 97% of coal matrix (pyridine insoluble <2% of coal), but its average aromatic
cluster size is supposed to have been reduced somewhat due to the nature of the reaction
among coal, NaOH and ethanol. According to Makabe and Ouchi (8), the reaction slightly
hydrogenates aromatic rings in coal under our experimental conditions. In any event,
our observations on two separately prepared CDL's indicate that the size of the average
aromatic cluster of the hvb coal is larger than 2.2, but not much different from 2.2.

The agreement in R_A/#cl between HVL-P and SP-300 suggest that large aromatic
clusters like those (R_A/#cl = 3.4) in Resid of HVL-P should exist in SP-300, i.e.
most probably in Fraction K. Comparison of the structural parameters of SP-300 with
those of SP-320 helps clarify this point. The large difference in R_A/#cl between
SP-300 and SP-320 is directly related to the question of the large aromatic clusters.

The difference in R_A/#cl is due to the conversion of Fraction K to a portion of
Fraction J' and Fraction K' as revealed by their R_A/#cl's and yields. Fraction J' con-
sists of two large portions, one coming from Fraction J and the other from Fraction K.
Still Fractions J' and J behaved similarly in a strong basic solution as described in
their preparation, and they have similar R_A/#cl and molecular weight (based on an
estimation of a separate conversion of J to a portion of J'). This indicates that
there was a portion of K which was similar to Fraction J in chemical structure, and
which was different from the rest of K: the two portions are termed Fractions K_J and
K_K respectively. Thus it is most likely that J and K_J experienced a similar transfor-
mation to become part of J'. In the conversion to J', apparently R_A/#cl of J was not
changed, and so was not that of K_J. Then the large change of R_A/#cl between SP-300
and SP-320 is due to a large change of the same parameter between K_K and K'.
R_A/#cl of K_K was large, but it reduced to that of K' upon the hydrogenation of NaOH/
ethanol reaction.

Model compound studies by Ross and Blessing (11) support this interpretation. They
observed that clusters consisting of single aromatic ring were not hydrogenated in a
reaction with KOH/methanol at 400°C for 30 minutes, but a cluster containing three fused
aromatic rings underwent hydrogenation. Estimation of R_A/#cl of K_K came out to be 3.4,
which is the same as that of Resid in HVL-P. The large decrease in R_A/#cl, from 3.4
(for K_K) to 1.4 (for K') upon hydrogenation suggests that the aromatic rings in the
clusters of K_K were mostly cata-condensed. Thus considerable amounts of polynuclear
aromatic clusters were observed in HVL-P and SP-300 which were supposed to retain most
of skeletal structure of the hvb coal.

Recently Whitehurst (12) and Farcasiu (13) reported that there is no significant
amount of large aromatic clusters in coal. Their coals and experimental method were
different from ours, but most notably their determination of the size of aromatic
clusters was semi-quantitative (13). Although their conclusion might hold with the
particular coals they examined, our findings support the conventional view that most
bituminous coals contain considerable amounts of polynuclear aromatic clusters.

These observations lead to the conclusion that there were originally three classes
of average aromatic clusters in terms of their size in the hvb coal. Two of them have,
on the average, 1.9 and 1.3 aromatic rings per cluster, and they were collected in
Fractions I' and J'. The third class has, on the average, 3.4 or more aromatic rings
per cluster, and was collected in Fraction K mixed with the precursor of J'. The
average size of the third class of clusters is expected to be larger than 3.4 since
hydrogenation of the aromatic clusters is suspected as discussed previously. Now
we will examine how these three classes of aromatic clusters would be further depolymer-
ized.

The findings with SP-300 and SP-320 substantiate the assumption made earlier,
i.e. that the aromatic double bonds experienced little change, if any, in the liquefaction

process in producing HVL-P. In the process, non-aromatic bonds between aromatic clusters in the coal were broken almost completely. Considering the milder reaction conditions in producing SP-300 and the same $R_A/\#cl$ of HVL-P and SP-300, further treatment of SP-300 in the liquefaction process would result in a complete depolymerization of SP-300 yielding a product similar to HVL-P. There are a couple of non-aromatic bonds linking aromatic clusters in SP-300 as revealed by $\#cl$.

The comparison of structural parameters which are shown in Tables 1 and 2 provides detailed information on the conversion of SP-300 to completely depolymerized product. The three fractions of SP-300, however, were insufficiently depolymerized to draw useful information from their structural parameters. Instead the structural parameters of Fractions I' and J' were examined since Fractions I, J and K_J were converted to Fractions I' and J'. The numbers of aromatic rings, R_A's, of I' and J' are already smaller than that of Resid in HVL-P. Thus upon further depolymerization, Fractions I' and J' could become Light, Middle or Heavy such as those in HVL-P. According to R_A and $\#cl$, 80% of J' will become Light or similar fraction in HVL-P (the predicted value is 17% of MAF coal, compared to 15% of Light plus light liquid). The rest of J' will become Heavy. Likewise, 70% of Fraction I' will become Middle/Heavy (the predicted value is 21%, compared to 17% of actual yield). The rest of I' will become Reside. Also the rest of SP-300, Fraction K_K, could become Resid/Char since both K_K and Resid have the same $R_A/\#cl$ (the predicted value came out to be the same as the actual yield, 35%). Taking account of the paraffinic material removed, 4%, and the loss, 5%, in preparing HVL-P, the predictions agree well with the actual yields.

The quantitative convertibility of SP-300 to HVL-P fractions further substantiates that the skeletal structures (or aromatic bonds) of coal were conserved during the liquefaction process as well as during the solubilization process at 300°C. Therefore the component groups A, B and C in HVL-P can be visualized as structural units of the coal. Almost all structural units were collected in SP-300 and they were grouped into three (Figure 2). The structural units in the first group, X, have one to two aromatic rings, and they are connected to each other by non-aromatic bonds. Although our data revealed that the linkages exist, their nature has not been studied yet. The structural units in the second group, Y, have two to three aromatic rings, and the third group consists of structural units having, on the average, four or more aromatic rings. Thus, the particular hvb coal has been characterized in terms of major structural units and their distribution. The same data analyzed so far provide valuable information also on the reduction of molecular size during the liquefaction, weak bonds, and the hydrogenation of aromatic clusters in coal, and this will be reported elsewhere.

Conclusion

A new characterization scheme for CDL has been devised based on the assumption that coal liquefaction is basically a depolymerization process. This scheme was instrumental in disclosing the following structural features of a hvb coal and its liquids:

(1) A CDL (HVL-P), produced at 500°C with very short residence time, was almost completely depolymerized, i.e., essentially all linkages between aromatic clusters were broken, and consisted of three major component groups, A, B and C. The components in Group A had mostly one aromatic ring, those in Group B two to three fused aromatic rings and those in Group C four or more fused aromatic rings. The fused aromatic rings have attachments such as naphthenic rings and aliphatic side chains. The three groups apparently are not convertible to each other under the liquefaction conditions used, and therefore, must have been produced from three different structural units in coal.

(2) A solubilization product (SP-300), obtained in a reaction with NaOH/ethanol at 300°C, revealed that it was less depolymerized than HVL-P, but the size of average aromatic cluster was the same, 2.2 aromatic rings per cluster, as that of HVL-P. SP-300 consisted of three classes of average aromatic clusters having 1.3, 1.9 and 3.4 aromatic rings per cluster. The distribution of the clusters was found by examining another solubilization product (SP-320)

prepared at 320°C. The aromatic rings of the large clusters appear to be cata-condensed.

(3) The clusters containing 1.3 and 1.9 aromatic rings per cluster are convertible to smaller species like Groups A and B in HVL-P, while the larger clusters of 3.4 aromatic rings will become Group C in HVL-P.

(4) The three groups of HVL-P were identified as the three major structural units of coal, and their distribution in the hvb coal was estimated from the examination of SP-300 and SP-320

These findings are unique to the characterization scheme for CDL. The results of this characterization of coal could be related to product potential in liquefaction, solvent refining and pyrolysis of coal. Taking into account the heterogeniety of coal and its inaccessibility by analytical means, the present approach appears to be a practical, useful way to characterize the chemical structure of coal. The same approach will be utilized with other coals which can be solubilized to further substantiate this method.

References

(1) Lowry, H.H., Ed. Chemistry of coal Utilization, Supp. Vol., John Wiley and Sons, New York, 1963.

(2) Van Krevelen, D.W., Coal, Elsevier Publishing Co., New York, 1961.

(3) Friedel, R.A., Ed. Spectrometry of Fuels, Plenum Press, New York, 1970.

(4) Larsen, J.W., Ed. Organic Chemistry of Coal, ACS Symposium Series 71, Am. Chem. Soc., Washington, D.C., 1978; Vahrman, M. Chem. Bit. 8, 16, 1972.; McIntosh, M.J., Fuel 55, 59, 1976.; Wiser, W.H., Anderson, L.L., Qader, S.A., and Hill, G.R., J. Appl. Chem. Biotech. 21, 82, 1971.; Gould, R.F., Ed. Coal Science, Adv. in Chem. Series 55, Am. Chem. Soc., 1966.; Neavel, R.C., Preprints, Div. of Fuel Chem., Am. Chem. Soc., 24 (1) 73, 1979.

(5) Farcasiu, M., Fuel, 56 9, 1977.; Given, P.H., Cronauer, D.C., Spakman, W., Lovell, H.L., Davis, A., and Biswas, B. Fuel, 54, 40, 1975.; Schultz, H. and Mima, M.J., Preprints, Div. of Fuel Chem., Am. Chem. Soc., 23 (2) 76, 1978.

(6) Wood, R.E., and Wiser, W.H., Ind. Eng. Chem., Process Res. Devel., 15, 144, 1976.

(7) Zilm, K.W., Pugmire, R.J., Grant, D. M., Wood, R.E., and Wiser, W.H., Fuel, 58, 11, 1979.

(8) Makabe, M., and Ouchi, K. Fuel Proc. Tech., 2 131, (1979).

(9) Chung, K.E., Anderson, L.L., and Wiser, W.H., Fuel, accepted for publication.

(10) Chapter XXII in Reference (2).; Clutter, D.R., Petrakis, L., Stenger, R.L., Jr., and Jensen, R.K., Anal. Chem. 44 (8) 1395, 1972.; Kanda, N., Itoh, H., Yokoyama, S., and Ouchi, K., Fuel, 57, 677, 1978.

(11) Ross, D.S., and Blessing, J.E. Preprints, Div. of Fuel Chem., Am. Chem. Soc., 24 (2), 125 (1979).

(12) Whitefurst D.D., Organic Chemistry of Coal, Ed. by Larson, J.W., ACS Symposium Series 71, Am. Chem. Soc., Washington, D.C. 1978, p. 1.

(13) Farcasiu, M., Preprints, Div. Fuel Chem., Am. Chem. Soc., 24 (1) 121, 1979.

TABLE 1

Analytical Data on HVL-P and Its Fractions

	Yield, Wt%	Mol. Wt.	R_A	R_N	#cl	f_a
HVL-P	100 (92.5)*	258 (268)	2.4 (2.4)	0.8 (0.9)	1.1 (1.1)	0.63 (0.60)
Light	19.2	183	1.2	0.6	1.0	0.55
Middle	15.7	210	1.6	0.7	1.1	0.58
Heavy	17.6	272	2.4	1.3	1.0	0.59
Resid	40.0	396	4.4	1.2	1.3	0.68

*Calculated from those of the four fractions.

TABLE 2

Structural Parameters of the Solubilization Products

	Yield*	Mol. Wt.	R_A	R_N	#cl	f_A	R_A/#cl
SP-300**	85.7	843	5.6	3.9	2.6	0.52	2.2
Fraction I	23.9	777	5.0	3.3	2.7	0.52	1.9
J	9.1	643	3.4	3.4	2.5	0.53	1.4
K	52.7	930	6.6	4.4	2.6	0.51	2.5
SP-320**	76.5	520	3.2	2.4	2.1	0.52	1.5
Fraction I'	26.6	478	3.2	2.3	1.7	0.55	1.9
J'	23.8	444	2.4	2.0	1.8	0.50	1.3
K'	26.1	690	4.4	3.1	3.1	0.52	1.4

*Weight % of coal (MAF)

**The parameters were calculated from the three fractions.

Structural Units X (39 mole %)

Structural Units Y (32 mole %)

Structural Units Z (29 mole %)

Figure 2. Structural Units Comprising
A hvb Coal

*Linkages exist but were not identified.

Light   Middle   Heavy   Resid

A   B   C

$C_{12.4} H_{16.3} O_{0.63}$

$C_{14.7} H_{18.4} O_{0.67}$

$C_{19.5} H_{22.1} O_{0.75}$

$C_{28.8} H_{29.9} O_{1.0}$

Figure 1. Sketches of Possible Structures of HVL-P
Fractions.

STRUCTURAL CHARACTERISTICS OF VITRINITES

SWADESH RAJ

Ebasco Services Incorporated
Two Rector Street
New York, New York 10006

INTRODUCTION

It is generally accepted that the various petrographic constituents of coals are derived largely from partly decayed organs of the higher plants and the chemical substances in them. Lignin, in particular, is thought to be an important part of the input to coalificatiion processes both in pre-served woody tissue and after the micorbial action. The nature of the sub-stances from which coals are derived are fairly well known. However, the chemical structures that they give rise to in coals are poorly understood. It was thought worthwhile to undertake a structural study of a set of vitrinite-rich coals (ie, derived from woody tissue), using experimental approaches that would assist in evaluating the extent to which lignin struc-tures are still recognizable after coalification. A reductive degradation method of Burges et al (1), which has previously revealed the presence of lignin-derived phenols in the humic acids of soils, was adopted. Since coals of higher rank than lignites do not contain humic acids, humic-acid-like materials were generated in high yields (80 - 110 percent) by a mild oxidation (2) using aqueous performic acid and the products subjected to the reductive degradation.

Paleobotanic studies show that the main types of plants that contributed to coal formation in the Carboniferous were primitive gymnosperm, tree ferns, seed ferns and club mosses. In the other main eras of coal formation, the Cretaceous and the Tertiary, the source plants were angiosperms of the modern type. It is observed that there is likely to be a significant spread in some structural features of the lignin and flavonoids in such a wide range of plant types. Therefore, geological history is also considered a potentially important factor in determining structural characteristics of vitrinites. Two peat samples, three lignites and thirty-eight subbituminous and bitu-minous coals were studied. The mixtures of phenols and phenolic acids ob-tained as trimethylsilyl ethers and esters were analyzed by gas chromatography/mass spectrometry.

EXPERIMENTAL INVESTIGATION

Selection of Coal Samples

For this study three sets of coals from different geological provinces were selected. These coals are rich in vitrinite plus pseudovitrinite (70 - 90 percent), and cover a wide range of rank. Ten coals each from Eastern and Interior provinces and fifteen coals from Rocky Mountain province were se-lected. Three lignites were selected from Texas and North Dakota. Two peat

samples were taken from the Southern Everglades of Florida. Details on the
analysis of selected peat, lignitic, subbituminous and bituminous coal samples
are given in Reference (3).

Experimental Method

The oxidation of coal by performic acid was carried out under con-
trolled conditions and the temperature was maintained at 50 - 55°C. Humic
acids were extracted from peats and lignites with 0.5 N NaOH and from oxi-
dized coals with 1 N NaOH. The washed and dried humic acids were dissolved
in NaOH, treated with 3 percent freshly prepared sodium amalgam, and the
solution was heated in an oil bath to temperatures of 110 - 115°C for 4 -
5 hours. The resulting phenols and phenolic acids were precipitated and
extracted by centrifugation with ether and methylene chloride. The solvents
were removed and the residues were treated with sylol HTP reagent under the
specified conditions for converting phenols and phenolic carboxylic acids
to their corresponding ethers and esters. The trimethyl ethers and esters
were analyzed by gas chromatography with and without coinjection. A few
of the identifications were made by Bimer et al (4) by gas chromatography
with coinjection of standards. With the wider range of coals and with a
wider set of standards more compounds were identified using GC/MS/Computer
System. Experiments showed OV 101 Column Packing (3 percent on 80/100 mesh
supelco port) to be the most effective for GC and GC/MS of the six packings
tested. The GC/MS instrument was provided with a data system. The data
system was used to subtract the mass spectrum at the foot of each peak just
before it began to elute, or just after the elution, from the spectrum re-
corded as the maximum of the peak was eluted. The raw MS data, described
above, were reported for standards and unknowns as printouts tabulating m/e
values and relative intensities. The comparisons were made by visual in-
spection of the printed data and the retention times.

EXPERIMENTAL RESULTS

It is impracticable to reproduce here all the chromatograms and all
the mass spectra obtained. Most of them are illustrated in Reference (3).
It is observed that humic acids obtained both by the extractions of lignites
and the oxidatation of the insoluble residues, and the humic acids obtained
from most (but not all) of the coals from the Rocky Mountain Province, gave
poorly resolved chromatograms, while those from the Carboniferous coals of
Interior and Eastern Provinces gave chromatograms where resolution ranged
from reasonable to excellent. The products from the peat humic acids showed
moderately good resolution. Taking an overview, 18 of 43 samples studied
showed poor resolution.

There are a number of difficulties in discussing the compounds iden-
tified and assessing their significance. Humic acids are poorly defined
substances of diverse origin, and their structures are unknown. In order
to facilitate discussion of the distribution of compounds identified, all
of the compounds partially or completely identified are listed in Table 1-
3, where the coals from which they come are classified partly by rank and
partly by the province. In each set of tables, the compounds are listed
as far as possible in order of increasing complexity.

In Table 1 are presented the phenols and acids whose structures are simple or nonspecific about their origin. Table 2a contains compounds that appear to have been derived from the A ring of flavonoids. In Table 2b are compounds of more complex structure with a very clear relationship to the breakdown products of lignin and B ring of flavonoids. Table 3 lists relatively complex compounds which again may have had a biological origin, but this cannot be proved; for many of them the substitution pattern in the benzene ring has not been identified. What is shown in the tables is the freqency of occurrences of the various compounds. At the head of each column of the tables is shown the total number of samples of each class studied, and against the name of each compound is shown the number of reaction products in which it was identified.

Throughout the study, a number or relatively large peaks could not be matched with the Standards available, and no more than the general character of the Structure could be inferred from the mass spectra. These peaks were scanned for negative as well as positive information. The principle conclusions arising from the examination of unidentified peaks were as follows:

1.   A majority of the large unidentified peaks represented phenols or phenolic acids.

2.   Some evidence of the presence of biphenyl groups was seen.

3.   In each chromatograms presence of hydroxy pyridines is seen.

4.   No evidence of the presence of Sulfur compounds was seen.

5.   Some mass spectra indicate the presence of either linkages (other than methoxyl) and of Carbonyl compounds.

DISCUSSION OF RESULTS

The most striking result of the whole study is the presence of cinnamic acid, which was found in 42 out of the 43 materials analyzed; the one product that did not contain cinnamic acid did contain the corresponding alcohol. The acid is found in a region of the chromatograms where the peaks rise directly from the baseline in almost all cases, and the peak corresponding to it was almost always sharp and intense. In addition, substances closely related to it were found in a few products, with the aliphatic side chain in a different state of oxidation, ie, not as $-CH=CH-COOH$ but as $-CH_2.CO.COOH$ or $-CH_2.CH_2.COOH$ or $-CH_2.CO.CH_2OH$. However, cinnamic acid is of common occurrence in plants as a biosynthetic precursor to lignin, flavonoids and phenylalanine, so that it could have entered peats as such and be incorporated into peat humic acids.

There is also present in many samples a group of compounds related to p. hydroxycinnamic acid (or p. coumaric acid). Again the side chain is in various states of oxidation ($-CH=CH-CH_2OH$, $-CH_2.CO.COOH$, $-CH_2.CH_2.COOH$). p. Coumaric acid itself is the most abundant of these, being found in about

half the products from subbituminous and bituminous coals, but only in one of the lower rank materials. On the other hand, p. hydroxybenzoic acid, which can be derived from coumaric acid and related compounds by oxidation of the side chain, was found in almost all of the low rank materials and in rather less than half of the products from the higher rank coals.

There are a large group of compounds related to 3-methoxy-4-hydroxy-cinnamic acid (ferulic acid). This substitution pattern is the most abundant in the lignin of Gymnosperms and in some less highly evolved plants such as the Lycopods, but is found also in Angiosperms. Vanillin (3-methoxy-4-hydroxy-benzaldehyde), formed in peats by microbial oxidation of ferulic acid was found in every one of the low rank materials studied, in 12 out of 15 samples from the Rocky Mountain Province, and in about one-half of those from the other provinces. In addition, the related compound, vanillic acid was found to be quite abundant. Ferulic acid itself, and caffeic acid (3,5-dihydroxy cinnamic acid) were each found in about 40 percent of the samples; a sample that contained one in general did not contain the other. Oddly enough, caffeic acid is the only substance in this group that has had the original 3-methoxy substituent demethylated to hydroxy. The other substances in this group contain the aliphatic side chain in various states of oxidation, of greater variety than was found with the compounds related to coumaric acid ($-CH_2.CO.CH_2OH$) $-CH_2.CO.COOH$, $-CH_2.CH_2.CHO$, $-CH_2.CH_2.CH_2OH$ and $-CHOH.CHOH.COOH$.

The final group of substances related to lignin have the 1, 3, 4 and 5 substitution pattern in the benzene ring. As with the groups already discussed, the side chain was found in a variety of oxidation states. Again only one demethylated derivative was found 3, 4, 5-trihydroxy cinnamic acid. What might be termed the parent compound, 3, 5-dimethoxy-4-hydroxy cinnamic acid, was found in 11 samples which was entirely restricted to the higher rank materials. Syringic acid and syringaldehyde, in which two of the carbon atoms in the aliphatic chain have been removed by oxidation, were the most frequently found members of this group (19 and 13 samples respectively), and their occurrences were fairly evenly distributed over all classes of coals, including the peats.

<div align="center">CONCLUSIONS</div>

By no means all of the substances that gave peaks on the chromatograms were identified, but a careful scrutiny of the data showed that identifications made were reasonably certain. The products derived from the Carboniferous coals of the Interior and Eastern Provinces were markedly less complex mixtures, and the degree of resolution was considerably better. From the results there are a number of important implications for understanding the chemistry of vitrinites. These may be summarized as follows:

1. Many benzene rings in vitrinites bear not only an OH group but often one or two methoxy groups as well; occasionally a second OH group may be present instead of methoxy. This would explain, among other things, the difficulty of sulfonating or nitrating vitrinites without accompanying oxidation.

2. Methoxyl groups survive in vitrinites to a considerably higher
   level of rank than previously reported.

3. Bicyclic and polycyclic aromatic ring systems, other than biphenyl,
   appear to be less frequent. It is possible that most of the
   polycyclic structures from coals accumulated in the ether-insoluble
   material.

4. The structure of vitrinites, even of High Voltatile A Bituminous
   rank, appears to be similar to that of lignin, in being based to
   an important extent on phenyl propane and phenyl methane skeletons.

5. Olefinic double bonds are abundant in vitrinite structures as such
   or they are generated by the degradation processes used, in a manner
   difficult to envisage at this time.

The conclusions are consistent with a feasible interpretation of the
X-ray scattering data of Hirsch (5). Further, it is also consistent with
the conclusions of Montgomery et al (6) and of Chakrabartty et al (7) on
their studies of the products of severe oxidation of coals.

ACKNOWLEDGEMENTS

REFERENCES

1. Burges, M.A., Hurst, H.M. and Walkden, S.B., Geochim et Cosmochim
   Acta 28, 1547, (1964).

2. Given, P.H., Brown, J.K., Lupton, Vera and Wyss, W.F., Proceedings of
   Institute of Fuel Conference, "Science in the Use of Coal," 38, 537
   (1958).

3. Raj, S., Ph.D. Thesis, The Pennsylvania State University (1976).

4. Bimer, J., Given, P.H., and Raj, S., ACS Symposium Series, No. 71,
   Organic Chemistry of Coal, (1978).

5. Hirsh, P.B., Phil. Trans Roy. Soc. (252A), 68 (1960).

6. Montgomery, R.S., Holly, E.D. and Gohlke, Fuel (35), 60 (1956).

7. Chakrabartty, S.K. and Berkowitz, N. Nature (Lond.), (1976).

TABLE 1

Simple Phenols and Acids Identified

Compound	Direct Humic Acid		Humic Acid from Oxidized Coals			
	2 Peats	3 Lignites	3 Lignites	15 Rocky Mountain Province Coals	10 Interior Province Coals	10 Eastern Province Coals
Acetic Acid					1	1
Propionic Acid					1	1
Benzoic Acid	2	1	1	2	1	3
Phenol	2	3		3	5	4
p-Cresol	2	1	1	12	2	
o-Methoxy Phenol	2	2	2	3	2	
m-Methoxy Phenol	2		2			
Hydroquinone	1	1				
m-Hydroxy Benzoic Acid		1		3	1	1
Catechol	2	2		7	5	3

TABLE 2a

Phenols Identified Having Biological Associations
(A-ring of Flavonoids)

Compound	Direct Humic Acid		Humic Acid from Oxidized Coals			
	2 Peats	3 Lignites	3 Lignites	15 Rocky Mountain Province Coals	10 Interior Province Coals	10 Eastern Province Coals
Resorcinol	2	1		7	2	3
Phloroglucinol	2			2	1	1
2-Methyl Resorcinol		1		3	4	5
2,4-Dihydroxy Toluene	1	3	1	7	3	5
o-Hydroxy Benzoic Acid			2	5	2	1
2,4,6-Trihydroxy Benzoic Acid	1	1	1	1	1	1
2,4,6-Trihydroxy Toluene					1	5

TABLE 2b

Phenols Identified Having Biological Associations
(Lignin and its Precursors; A-ring of Flavonoids)

Compound	Direct Humic Acid		Humic Acid from Oxidized Coals			
	2 Peats	3 Lignites	3 Lignites	15 Rocky Mountain Province Coals	10 Interior Province Coals	10 Eastern Province Coals
Cinnamic Acid	2	3	3	14	10	10
Cinnamic Alcohol	1	1	1	1		
Phenyl, 3-Pyruvic Acid				1	2	2
Phenyl, 3-Propionic Acid				2	1	1
Phenyl, 3-Pyruvic Alcohol						
p-Hydroxy Benzoic Acid	2	3	3	5	4	3
p-Coumaric Acid			1	6	4	5
p-Coumaryl Alcohol	1			1		2
p-Hydroxy Phenyl, 3-Pyruvic Acid		1	1	2	3	2
p-Hydroxy Phenyl, 3-Propionic Acid				3		
Pyrogallol	2	1		1	2	2
Gallic Acid				1	1	1
Vanillin	2	3	3	12	5	1
Vanillic Alcohol				2	1	6
Vanillic Acid	1	2	1	5	5	3
Acetovanillone	1			4	1	1
Ferulic Acid	1		1	4	3	7
Caffeic Acid	1	1	1	6	4	6
3-Methoxy, 4-Hydroxy Phenyl, 3-Pyruvic Alcohol		2	1	3	2	4
3-Methoxy, 4-Hydroxy Phenyl, 3-Pyruvic Acid			2	3		4
3-Methoxy, 4-Hydroxy Phenyl, 3-Propion-Aldehyde		1		2	2	3

Compound	Direct Humic Acid		Humic Acid from Oxidized Coals			
	2 Peats	3 Lignites	3 Lignites	15 Rocky Mountain Province Coals	10 Interior Province Coals	Eastern Province Coals
3-Methoxy, 4-Hydroxy Phenyl, 3-Propanol				1		
3-Methoxy, 4-Hydroxy Phenyl, 3-Glyceric Acid	1	1	1	3	1	
Dehydrovanillone				2	1	
Syringic Aldehyde	1	1	1	5	3	2
Syringic Alcohol				3	2	4
Syringic Acid	2	1	1	7	5	3
3, 5-Dimethoxy, 4-Hydroxy Phenyl, 3-Pyruvic Aldehyde		2	1		1	4
3, 5-Dimethoxy, 4-Hydroxy Phenyl, 3-Propionic Acid				1		
3, 5-Dimethoxy, 4-Hydroxy Phenyl 3-Glyceric Acid					1	
3, 5-Dimethoxy, 4-Hydroxy Phenyl 3-Pyruvic Acid	1	1		2		
3, 5-Dimethoxy, 4-Hydroxy Cinnamic Acid				3	5	3
x, y-Dimethoxy Cinnamic Alcohol					1	
x, y-Dihydroxy Cinnamic Aldehyde					3	2

258

TABLE 3

Complex Phenols Identified of Unknown or Uncertain Biological Associations

	Direct Humic Acid		Humic Acid from Oxidized Coals			
Compound	2 Peats	3 Lignites	3 Lignites	15 Rocky Province Coals	10 Interior Province Coals	10 Eastern Province Coals
2,6-Xylenol		2	2	9	4	5
3,5-Dihydroxy Toluene				1	1	1
Hydroquione	1					
x,y-Dimethoxy Phenol					2	1
x-Phenyl Phenol					2	1
x,y-Dihydroxy Benzophenone		2	1			
x-Methoxy Phenyl, 3-Propionic Acid				6	1	1
x-Methyl Benzoic Acid				1		1
x-Methoxy Benzoic Acid				1	1	1
2,5-Dihydroxy Benzoic Acid				2	2	3
x,y-Dimethoxy Phenyl, 3-Propionic Acid				1		
x,y-Dimethoxy Cinnamic Alcohol					1	
x,y-Dihydroxy, Monomethyl Benzoic Acid					3	1
v,x-Dimethoxy, Y,Z-Dihydroxy Benzoic Acid				2	1	
v,x-Dimethyl, Y,Z-Dihydroxy Benzoic Acid				2	1	
1,2,4-Trihydroxy Benzoic Acid	2					
Saligerum		2		3		

Thermolysis and Oxidation of the Alberta Oil Sand Bitumen

K.N. Jha, D.S. Montgomery and O.P. Strausz

Hydrocarbon Research Centre
Department of Chemistry
University of Alberta
Edmonton, Alberta
Canada T6G 2G2

INTRODUCTION

The composition and the rates of evolution of light gases and volatile materials from Athabasca and Cold Lake oil sand bitumen and their separated fractions have been described as a function of temperature.[1-3] From the estimation of the Arrhenius parameters for product formation it was concluded that both these reservoirs are currently undergoing a slow but measurable thermal decomposition even at the formation temperature. The activation energies for the formation of products for the whole oil sand system were low, ranging between 6 and 26 kcal/mol, indicating the catalytic effects of mineral matter present in the oil sand. Previous work suggests a common origin for these oils, and our own results[1-3] suggested similar thermal diagenetic histories for the Athabasca and Cold Lake oil sand deposits. Similar studies have now been conducted on the Peace River oil sand to gain deeper insight into the relationships between this oil and the other two oil sands.

Preliminary results on the kinetics of consumption of molecular oxygen in the thermolysis of the Athabasca oil sand, extracted bitumen, asphaltene and maltene have shown that the rate of thermolysis of each product was substantially increased in the presence of molecular oxygen and that the rate of depletion of oxygen followed first order reaction kinetics.[3,4] Exposure of the oil sand to oxygen resulted in a substantial increase in the asphaltene content of the sample.

These studies have been extended to include the effects of oxygen pressure and heating time on the yields of the products from the whole oil sand as a function of temperature in order to clarify geological processes such as the introduction of molecular oxygen into the bitumen via oxidizing ground water and weathering processes occurring at the oil sand outcrops or in piles of mined bituminous sand.

EXPERIMENTAL

The experimental details for the collection and analysis of gases and the volatile materials have been described previously.[1-3] The Peace River oil sand was received from Shell Canada Ltd., labeled OBS-5 Shell Cadotte OV, 4-21-85-18 W5 from a depth of 563-573 m. These samples were contained in split cores which had been exposed to air at some stage. The oil sands were manually homogenized before use for most of the experiments in order to obtain reproducible results.

The bituminous sands from the Saline Creek tunnel area of the Athabasca reservoir were used for the oxidation experiments. Bitumen was extracted from this oil sand and separated into asphaltenes and maltenes using standard techniques.[5] Trace amounts of clay and mineral matter present in these fractions were removed by centrifugation. Non-condensable gases at 77°K were analyzed by gc on a 2.4 m molecular sieve column and the gases volatile at 195°K but condensable at 77°K on a 4.6 m Porapak Q column. Since neopentane, acetone, propionaldehyde and carbon disulfide are unresolved on Porapak Q, this total fraction was trapped from the effluent and further analyzed on a 4.6 m tricresylphosphate column, on which excellent resolution was achieved.

RESULTS AND DISCUSSION

The composition and rates of the light gases evolved from the Peace River bituminous sand at 278, 298, 323, 343, 368, 388, 403 and 423°K are presented in Table I. The volatile material obtained up to 298°K, which is the formation

Table I. Composition of Gases Evolved from the Peace River oil sand as a Function of Temperature

Temperature (°K)	10^{-8} mol hr^{-1} kg^{-1} oil sand							
	278	298	323	343	365	388	403	423
Heating Time (hours)	5.5	5.5	5.5	5.2	3.0	2.0	2.0	1.0
Methane	0.62	0.85	1.4	7.6	20.7	80.1	165	577
Ethylene	n.o.[a]	0.10	10.2	12.7	7.9	24.3	35.8	43.4
Ethane	n.o.	0.03	0.58	6.1	3.2	8.9	20.1	50.5
Methanol	n.o.	n.o.	n.o.	0.11	4.3	11.7	11.6	16.1
Acetaldehyde	0.03	0.18	12.2	26.4	80.2	126	101	155
Propylene	0.10	0.11	10.9	11.6	15.6	37.2	62.6	156
Propane	n.o.	n.o.	1.8	4.2	22.2	12.6	34.7	357
i-Butane	n.o.	n.o.	0.09	0.9	11.6	7.9	20.8	151
i-Butene	n.o.	n.o.	6.3	6.2	8.7	27.5	50.3	124.5
n-Butane + Butenes	n.o.	0.13	0.78	3.0	7.4	17.0	21.8	86.7
Pentanes + Pentenes	17.7	26.4	6.7	13.0	65.8	112	170	609
C_6	7.3	9.8	2.7	6.2	10.9	24.9	38.0	119
Carbon monoxide	0.24	0.54	14.4	20.3	483	261	548	2,050
Carbon dioxide	143	500	3,260	6,820	24,300	13,400	26,800	101,000
Carbonyl sulfide	0.03	0.04	0.59	1.30	11.5	20.3	31.8	105

[a]Not observed.

temperature, are CH_4, C_2H_4, C_2H_6, CH_3CHO, C_3H_6, n-C_4H_{10}, 1- or 2-C_4H_8, C_5, C_6, CO, CO_2 and COS, and these are considered to be constituents present in the formation. Neopentane was not detected in these samples, in contrast to the Athabasca and Cold Lake bituminous sand.[1-3]

It is observed that a considerable similarity exists in the gases found to be present in the Peace River, Cold Lake and Athabasca deposits with the notable exception of neopentane, which is absent in the Peace River reservoir.[1-3] The formation temperatures for the Athabasca, Cold Lake and Peace River reservoirs are 278, 293 and 300°K, respectively. The yields of hydrocarbon gases - with the exception of methane - from three reservoirs at 343°K increase with increasing formation temperature.[3]

The yields of all materials after a given time are enhanced with increasing temperature, indicating that both thermolysis and desorption processes may be involved in determining the yield. The amounts of volatile materials evolved at 278°K are less from the Peace River bituminous sand than those from the Athabasca and Cold Lake samples.[1-3] However, the rates of increase of most of the products with rising temperature are higher in the former than in the latter.

The yields of products as a function of reaction time of Peace River oil sand were studied in detail at 423°K using homogenized bituminous sand samples. The homogenization process was done quickly to minimize additional contact of the bituminous sand with air. The results show that although the product yields increase with increasing reaction time, however, the rates of formation of some of the products actually decreased. This is illustrated for the cases of CH_4, C_2H_4, i-C_4H_8, CO and COS in Figure 1 where rates of formation could be estimated from the slopes of the curves. From these plots it appears that CH_4, CO and COS are primary

products while the principal origins of C_2H_4 and $\underline{i}\text{-}C_4H_8$ are secondary in nature.
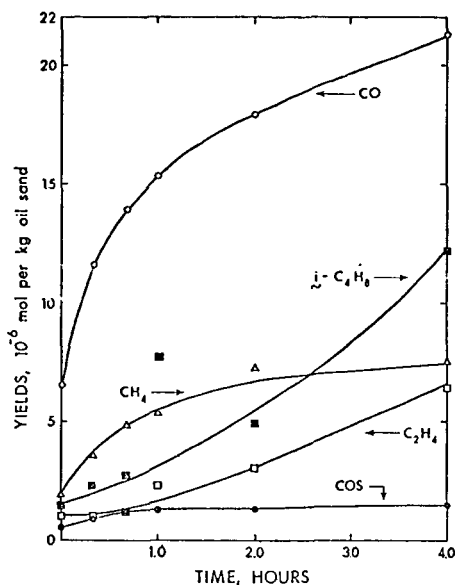

Figure 1. Yields of gases as a function of time in the Peace River oil sand at 423°K.

    Kinetic treatment of some of the data in Table I, i.e., plots of the logarithms of rates versus reciprocal temperatures yielded Arrhenius parameters which are listed in Table II. The corresponding values estimated from the Cold Lake and Athabasca data are included in Table II for comparison. The activation energies for the most of the product formation from Peace River oil sand are higher than those from Athabasca or Cold Lake samples. This implies that the former reservoir is more mature than the latter two. It is interesting to note, however, that the activation energy of 4.1 kcal/mol for ethylene formation from Peace River oil sand is much lower than those for Athabasca or Cold Lake, which are 11.8 and 12.4 kcal/mol, respectively. It must be pointed out that all the activation energies measured are very low, indicating that catalytic processes are involved. The rates of product formation at 278°K, calculated by extrapolation of the Arrhenius parameters, are included in Table II. These rates, which are small but significant even at 278°K, indicate that all these oil sand reservoirs of Alberta are presently undergoing similar thermal maturation processes.

    The distribution of the products and the values of the Arrhenius parameters for these oil sand formations support our earlier conclusion that these deposits have a common origin and a similar diagenetic history.[1-3,6]

    The yields of the volatile materials collected from Athabasca oil sand at 333°K in the absence and presence of oxygen are listed in Table III. In the absence of oxygen C_1-C_6 hydrocarbons, CH_3CHO, CO and CO_2 were detected. In the presence of oxygen acetone, propionaldehyde and carbon disulfide are produced in addition to the above compounds. It was observed that oxygen has an enhancing effect on the yields of every product except olefins. These results are in contrast to those

Table II. Arrhenius Parameters for the Thermolysis of Peace River (PR), Cold Lake (CL) and Athabasca (AT) Oil Sands

Product	A (mol hr^{-1} kg^{-1})			E_a (kcal/mol)			$R_{278°K}$ (mol hr^{-1} kg^{-1})		
	PR	CL	AT	PR	CL	AT	PR	CL	AT
CH$_4$	1.8×10^3	3.1	6.5	16.6	12.8	13.6	1.7×10^{-10}	3.1×10^{-10}	1.4×10^{-10}
C$_2$H$_4$	5.5×10^{-5}	3.8×10^{-1}	9.5×10^{-2}	4.1	12.4	11.8	3.3×10^{-8}	8.0×10^{-11}	5.1×10^{-11}
C$_2$H$_6$	5.3×10^1		1.2×10^{-3}	15.5		8.3	3.2×10^{-11}		3.5×10^{-10}
C$_3$H$_6$	7.1	9.6×10^{-2}	1.4	12.9	11.2	13.8	4.7×10^{-10}	1.7×10^{-10}	2.2×10^{-11}
i-C$_4$H$_8$	8.8×10^2		2.9×10^{-5}	17.3		6.8	2.2×10^{-11}		1.3×10^{-10}
ī-C$_4$H$_{10}$	5.5×10^1	5.5×10^{-6}	1.5×10^{-4}	14.8	5.1	8.3	1.3×10^{-10}	5.6×10^{-10}	4.5×10^{-11}
C̄O	7.6×10^3	1.4×10^{-1}	2.0×10^{-1}	16.7	9.4	8.8	5.5×10^{-10}	6.5×10^{-9}	2.4×10^{-8}
CO$_2$	1.1×10^2			9.8			2.1×10^{-6}		
COS	4.9×10^1	3.5×10^{-3}	9.1×10^{-2}	14.9	9.0	11.6	1.0×10^{-10}	3.3×10^{-10}	7.3×10^{-11}

Table III. Composition of Gases from the Oxidation of the Athabasca Oil Sand at 333°K[a]

Rates, 10^{-8} mol hr^{-1} kg^{-1} oil sand

Product	O$_2$		Product	O$_2$	
	Nil[b]	6.37 mmol[c]		Nil[b]	6.37 mmol[c]
Methane	0.18	0.26	Pentanes + Pentenes	0.55	0.23
Ethylene	0.41	0.12	C$_6$	0.10	0.12
Ethane	0.05	0.06	Acetaldehyde	0.06[d]	0.57
Propylene	0.39	0.14	Acetone	n.o.	0.17
Propane	0.01	0.04	Propionaldehyde	n.o.	0.10
i-Butene	0.01	0.03	Carbon monoxide	0.08	7.73
ī-Butene	0.27	0.05	Carbon dioxide	38.8	125
n̄-Butane	0.03	0.04	Carbon disulfide	n.o.	0.04
Neopentane	0.12	0.32			

[a] Each sample contained 200 g oil sand. [b] The sample was heated for 1846 hours. [c] The sample had an initial 411 torr pressure of oxygen and was heated for 1822 hours. [d] Not observed.

obtained at 403°K where oxygen has an enhancing effect on the yields of each product.[4]

The rates or ratios of rates of evolution of some of the gases at 403°K for 4 hrs heating time as a function of oxygen pressure are plotted in Figure 2. It is apparent from these plots that the rate of thermolysis increases with increasing pressure of oxygen; however, the rates of some products rise more rapidly than those of others.
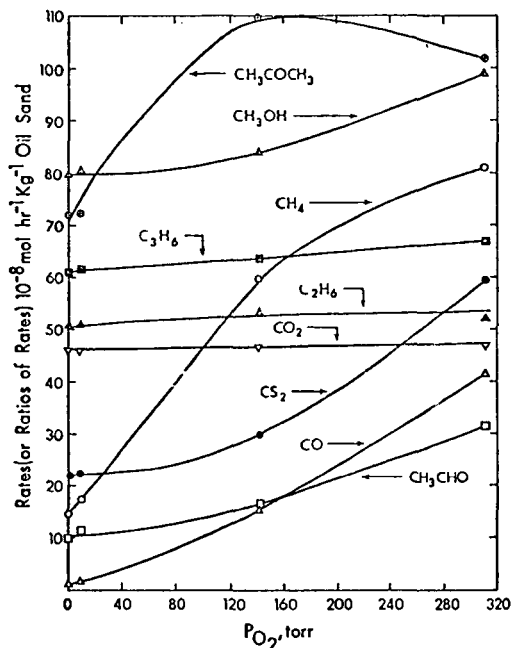

Figure 2. Rates or ratios of rates (based on the rate in the absence of $O_2 = 1.00$) in the thermolysis of Athabasca oil sands at 403°K as a function of oxygen pressure:

○, CH_4 (rates);

△, CO (rate ratios);

▽, CO_2 (rate ratios + 45);

□, CH_3CHO (rate ratios + 10);

●, CS_2 (rates + 20);

▲, C_2H_6 (rates + 50);

■, C_3H_6 (rates + 60);

⊕, CH_3COCH_3 (rates + 70) and

△, CH_3OH (rates + 80).

It has been observed that the rates of evolution of CH_4 and CO at 373°K are not appreciably affected in the presence of a few torr oxygen but are markedly enhanced at higher pressures. These results imply that either the product yields are insensitive to trace amounts of oxygen in the system or that the sample was already contaminated with oxygen during storage and handling.

The yields of a few typical products are plotted as a function of time in Figure 3. Those of CH_3CHO, CH_3COCH_3, C_2H_5CHO and CS_2 initially increase with increasing conversion of the bitumen, then decline, as secondary reactions begin to predominate. The trend in the CO production is not as clearly defined but it is highly improbable that such a stable molecule would undergo secondary reactions; very likely, its yield becomes constant as the precursors become depleted.

CH_3CHO, CH_3COCH_3 and C_2H_5CHO are typical products observed in the thermolysis of hydrocarbons in the presence of molecular oxygen and also have been observed to pass through a maximum with increasing conversion.[7-10] In these systems, however, CO is a minor product at low conversion and CO_2 is only detected at high conversions, of the order of 30%.[10] In contrast, even at very low conversions, CO and CO_2 are the most abundant products formed upon oxidation of oil sands, and the CO_2 yields are much higher than those of CO. It is tempting to conjecture that these
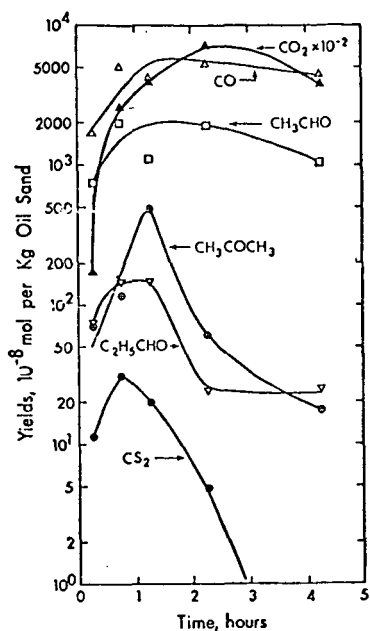
Figure 3. Yields of the thermolysis products of Athabasca oil sand in the presence of oxygen at 403°K as a function of time.
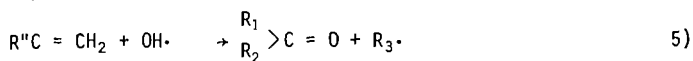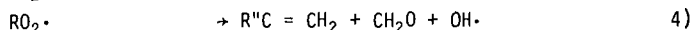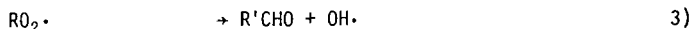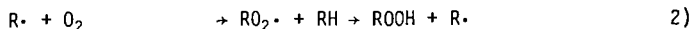
products are formed mainly, if not entirely, from carboxylic acids and aldehydes already present as constituents in the bitumen and that the other identified products are formed _via_ oxidation of hydrocarbon precursors; however, we have observed that the CO and CO_2 yields depend to some extent on the nature of the sample and its previous history and therefore much more work is needed before the reaction channels can be elucidated.

The oxidation of hydrocarbons by molecular oxygen involves a complex reaction network; however, it is commonly accepted that a chain mechanism is operative and that one of the first products formed is a hydroperoxide which may be oxidized further or decompose thermally, initiating new chains.[7-12]
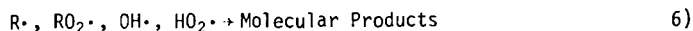
- initiation:

$$RH + O_2 \qquad \rightarrow R\cdot + HO_2\cdot \qquad\qquad 1)$$

- chain propagation:

$$R\cdot + O_2 \qquad \rightarrow RO_2\cdot + RH \rightarrow ROOH + R\cdot \qquad 2)$$

$$RO_2\cdot \qquad \rightarrow R'CHO + OH\cdot \qquad\qquad 3)$$

$$RO_2\cdot \qquad \rightarrow R''C = CH_2 + CH_2O + OH\cdot \qquad 4)$$

$$R''C = CH_2 + OH\cdot \qquad \rightarrow \begin{matrix} R_1 \\ R_2 \end{matrix}\!\!>\!C = O + R_3\cdot \qquad 5)$$

- chain termination:

$$R\cdot,\ RO_2\cdot,\ OH\cdot,\ HO_2\cdot \rightarrow Molecular\ Products \qquad 6)$$

265

Detailed discussions of this general mechanism have been presented in several publications.[7,8,10-11] This type of mechanism applies to pure hydrocarbons and its application to a complex system such as Athabasca oil sand is of very limited scope; moreover, it does not account for most of the CO_2 and CO yields evolved in this low temperature region, 278 to 403°K.

It should be noted that the quantities of CO and CO_2 evolved are the most sensitive indicators of the degree of oxidation of the sample and therefore can shed light on its previous history. For example, CO was demonstrably absent among the products evolved upon thermolysis of a fresh oil sand sample from the Athabasca reservoir, strongly suggesting that this deposit has not been exposed to air in the recent past.

ACKNOWLEDGMENTS

REFERENCES

1. Strausz, O.P., Jha, K.N. and Montgomery, D.S., Fuel (1977) 56, 114.
2. Jha, K.N. and Strausz, O.P., Preprints, Div. Fuel Chem., ACS, (1977) 22, 14.
3. Jha, K.N., Montgomery, D.S. and Strausz, O.P., "Oil Sand and Oil Shale Chemistry", Eds. Strausz, O.P. and Lown, E.M., Verlag Chemie Int., New York, (1978), 33.
4. Jha, K.N., Rao, P.M. and Strausz, O.P., Preprints, Div. Fuel Chem., ACS, (1978), 23, 91.
5. Selucky, M.L., Chu, Y., Ruo, T. and Strausz, O.P., Fuel (1977) 56, 369.
6. Jha, K.N., Gray, J. and Strausz, O.P., Geochim. Cosmochim. Acta, in press.
7. Sieg, L., "Low Temperature Oxidation", ed. Jost, W., Gordon and Breach Science Publishers, New York (1965), 191.
8. Drysdale, D.D. and Norrish, R.G.W., Proc. Roy. Soc. A., (1969), 308, 305.
9. Kovalev, G.I. and Denisov, Y.T., Neftekhimiya, (1976), 16, 457.
10. Baker, R.R., Baldwin, R.R., Everett, C.J. and Walker, R.W., Comb. and Flame, (1975), 25, 285.
11. Allara, D.L., Mill, T., Hendry, D.G. and Mayo, F.R., "Oxidation of Organic Compounds, Vol. II", Adv. Chem. Series, (1968), 76, 40.
12. Boboleva, S.P., Bulygin, M.G. and Blyumberg, E.A., Neftekhimiya, (1974), 14, 730.

The Reactions of Coal with
Transition Metal Halides

Herbert Beall

Department of Chemistry
Worcester Polytechnic Institute
Worcester, Massachusetts 01609

Introduction

Many studies(1) of the X-ray diffraction patterns of coal have
yielded the result that increasing coal rank results in increasingly
sharp diffraction patterns(2). Furthermore, as the rank limit is
approached the very high rank metaanthracites give diffraction with
essentially all of the features of a pattern obtained from graphite(3).
These results have led to the general acceptance of the model that
coalification involves the growth of polynuclear condensed aromatic
structures into graphite-like units(1,4). It is of interest to
determine if chemical properties of graphite are manifested by coal.
In particular, it is well-known that graphite will undergo reactions
with a variety of reagents to form intercalation compounds where the
graphite layers are separated to accommodate a variety of species
between them(5,6). It is therefore of interest to establish if such
intercalation compounds can be prepared from coal and, in fact, a
recent report very strongly supports that such compounds can be pre-
pared from coal and potassium(7). This paper describes attempts to
prepare coal intercalation compounds with the chlorides of iron(III),
chromium(III), and copper(II). Analysis of the results is by X-ray
powder diffraction. The 002 line in the X-ray powder pattern of
graphite is the strongest graphite line and represents the spacing
between planar polyaromatic layers of carbon. Formation of intercala-
tion compounds separates these carbon layers and affects this 002
line.

Results and Discussion

Initial experiments(8) were carried out in which anhydrous
iron(III)chloride ($FeCl_3$) was reacted with four different coals.
$FeCl_3$ was chosen for the initial studies because its intercalation
compounds with graphite are among the best known and most easily pre-
pared(5,6). The coals selected were the following: PSOC-379, Penn-
sylvania semi-anthracite (P&M'B'); PSOC-151, New Mexico high vola-
tile bituminous C (Lower Split of Blue); PSOC-240, Washington sub-
bituminous B (Big Dirty); and PSOC-247, North Dakota lignite (Noonan).
These four coals were treated directly with $FeCl_3$ after pulverization
and air drying at 120° and were also treated with $FeCl_3$ after a
demineralization(9) which involved washing with 10% HCl at 50°C for
18-24 hours followed by air drying at 120°. X-ray diffraction pat-
terns of the untreated and demineralized coals were essentially iden-
tical except that enhanced crystallinity of the demineralized samples
was evidenced by the shorter diffraction times needed to obtain equi-
valent diffraction patterns. PSOC-151, PSOC-247, and PSOC-240 showed
principally the 002 graphite line whereas PSOC-379 gave this line
strongly as well as other lines from crystalline matter.

In each of these six reactions with $FeCl_3$ approximately 1.0 g of
coal and 0.6 g of $FeCl_3$ were mixed and then heated to 230° for ten
minutes. No obvious evidence of reaction was observed and the final

products look similar to the coal starting material. Incorporation of the $FeCl_3$ into the coal is evidenced by the failure of the reaction products to react readily with water to form the yellow-brown hydrate which the unreacted $FeCl_3$ forms. The diffraction patterns of the coal-$FeCl_3$ products of PSOC-151 and PSOC-240 do not include the 002 graphite line which was prevalent in the coal starting material and this line is almost completely eliminated for PSOC-379. More rigorous conditions using 2 g of $FeCl_3$ per gram of coal and heating for 36 minutes at up to 250° were found to produce products where the 002 graphite line was eliminated for PSOC-379. The products under these more rigorous conditions were observed to be more gray and powdery than the starting coal. The more rigorous conditions required for PSOC-379 could be attributed to more extensive graphite-like structures in the semi-anthracite coal. Examination of the diffraction patterns of the PSOC-247(lignite)-$FeCl_3$ products gave ambiguous results with removal of the 002 graphite line evident only in the demineralized sample. However, the 002 line in the starting material is relatively weak.

A further observation is the appearance of diffraction lines attributable to $FeCl_2 \cdot 2H_2O$ in the patterns of some of the reacted samples. This evidence of reduction and hydration of the $FeCl_3$ was observed for the demineralized samples of PSOC-379, PSOC-151 and PSOC-247, and both dried and demineralized samples of PSOC-240. The nature of the material in the coal which was oxidized was not determined. The H_2O of hydration may have come from moisture still adsorbed on the hydrophilic surface of the coal which may have been rendered more hydrophilic by the demineralization process. Other sources of the H_2O are possible and cannot be overruled.

The demineralized PSOC-379 and PSOC-247 products with $FeCl_3$ were then washed with 10% HCl at 50° for 18 hours and subsequently dried in air at 120°. The diffraction patterns obtained from the samples after washing were identical to those of the coal samples prior to reaction with $FeCl_3$ except that a longer time seemed to be needed to obtain the same intensity of diffraction possibly indicating some breakdown of the crystallinity. Thus the reaction with $FeCl_3$ is largely reversible in these cases. Testing of the wash liquid obtained from these experiments with $K_3Fe(CN)_6$ solution gave a strong test for Fe^{++} in corroboration of the X-ray evidence above that $FeCl_2 \cdot 2H_2O$ is formed in the coal-$FeCl_3$ reaction.

Comparison experiments were run in which $FeCl_3$ was reacted with amorphous carbon powder (Acheson Graphite, Grade 38) which can be regarded as microcrystalline graphite. These experiments yielded observations which were parallel to those obtained with coal except that more $FeCl_3$ and more rigorous conditions were required to eliminate completely the 002 diffraction line of the amorphous carbon. The carbon would be expected to be able to intercalate more $FeCl_3$ than the much more hetereogeneous coal structure. Diffraction lines for $FeCl_2 \cdot 2H_2O$ were faintly discernible in the diffraction patterns of the carbon-$FeCl_3$ product and a distinct Fe^{++} test was obtained in the 10% HCl wash liquid. Presumably this can be attributed to adsorbed moisture on the carbon surface and oxidation of some of the carbon.

These experiments were extended to anhydrous chromium(III)-chloride ($CrCl_3$) and anhydrous copper(II)chloride ($CuCl_2$). Each of

these salts was reacted with demineralized PSOC-240 and dried PSOC-379 in an approximate ratio of 1.8:1 (g coal: g salt) at 250°. Acidic vapors were evolved in each reaction; the reaction with $CuCl_2$ resulted in removal of the 002 graphite line but the reaction with $CrCl_3$ did not. Examination of the coal-$CuCl_2$ product diffraction patterns did not yield perceptible lines for any material other than $CuCl_2$. Washing of the PSOC-379 product with 10% HCl resulted in the return of the diffraction pattern of the starting coal. It was noted that the PSOC-379 had been converted to an extremely fine powder in the course of reaction with $CuCl_2$ and then washing with 10% HCl. This would seem to be indicative of very extensive penetration of the $CuCl_2$ into the coal structure.

Further investigations involved the reactions of coal with the corresponding hydrated salts, $FeCl_3 \cdot 6H_2O$, $CrCl_3 \cdot 6H_2O$, and $CuCl_2 \cdot 2H_2O$. Demineralized and untreated samples of PSOC-379, PSOC-151, and PSOC-240 were reacted with approximately equal weights of $FeCl_3 \cdot 6H_2O$ at 215° for 3 minutes. Each of these mixtures was observed immediately to become liquid and chemical reaction was evidenced by bubbling which occurred for about one minute. At that point the mixtures suddenly solidified and were noticeably more grey in color than the starting pulverized coal. Disappearance of the 002 graphite line was observed in the reactions of the PSOC-379 samples with $FeCl_3 \cdot 6H_2O$ and this line was almost completely removed in the PSOC-151 and PSOC-240 reactions. All diffraction patterns of the reacted products showed that $FeCl_2 \cdot 2H_2O$ had been produced. Washing the products of demineralized PSOC-379 and $FeCl_3 \cdot 6H_2O$ with 10% HCl at 50° brought back the original demineralized coal diffraction pattern although with lines slightly weaker and slightly more diffuse. The liquid remaining from this washing gave a strong test for Fe^{++} again corroborating the formation of $FeCl_2 \cdot 2H_2O$ in the reaction. Parallel experiments with amorphous carbon resulted in virtual removal of the 002 diffraction line when the ratio of $FeCl_3 \cdot 6H_2O$ to carbon was about 2.5:1 (g:g). No $FeCl_2 \cdot 2H_2O$ lines were observed in the patterns from the carbon-$FeCl_3 \cdot 6H_2O$ product and the original carbon diffraction pattern could be returned by washing this product with 10% HCl at 50°.

Reactions of demineralized samples of PSOC-379 and PSOC-151 with $CrCl_3 \cdot 6H_2O$ and $CuCl_2 \cdot 2H_2O$ both resulted in removal of the 002 graphite lines in the coals. The ratio of coal to salt was about 1.25:1 (g:g) and the reaction conditions were 250° for nine minutes. Dehydration and evolution of acid vapors were evident with both salts; diffraction lines for anhydrous $CuCl_2$ were evident in the coal-$CuCl_2 \cdot 2H_2O$ product patterns. No diffraction lines for crystalline salts were evident in the products of the reactions of coal and $CrCl_3 \cdot 6H_2O$. The PSOC-379 diffraction pattern was returned when the products of each of the salts and this coal were treated with 10% HCl at 50°. This washing of the PSOC-379-$CuCl_2 \cdot 2H_2O$ product again gave back the coal in an extremely finely divided state as was the case in the reaction with anhydrous $CuCl_2$ (above). Comparison reactions in which $CrCl_3 \cdot 6H_2O$ and $CuCl_2 \cdot 2H_2O$ were reacted with amorphous carbon gave results which were generally parallel to the results of the reactions of these salts with coal except that more salt was needed to effect removal of the 002 line with $CuCl_2 \cdot 2H_2O$ and complete removal of this line was not achieved with $CrCl_3 \cdot 6H_2O$.

Experimental

Reagents were obtained from standard commercial sources and coal samples were donated by Pennsylvania State University. Powder diffraction patterns were recorded on film using FeKα radiation.

Acknowledgment

References

1. D. W. van Krevelen, Coal, Elsevier, Amsterdam, 1961.

2. R. Westrik, unpublished results reported in (1).

3. M. Mentser, H. J. O'Donnell, and S. Ergun, Fuel, 41, 153(1962).

4. H. L. Retcofsky, in B. R. Cooper, Ed., Scientific Problems in Coal Utilization, p. 79-99, U. S. Department of Energy, 1978.

5. W. Rudorff, Advances in Inorganic Chemistry and Radiochemistry, 1, 223(1959).

6. G. R. Henning, Progress in Inorganic Chemistry, 1, 125(1959).

7. L. Lazarov, I. Roshkov, and S. Angelov, Fuel, 57, 637(1978).

8. H. Beall, Fuel, 58, 319(1979).

9. R. G. Jenkins, S. P. Nandi, and P. L. Walker, Jr., Fuel, 52, 288(1973).

Thermal Decomposition of Aromatic Substances

R. E. Miller and S. E. Stein

Department of Chemistry, West Virginia University, Morgantown, WV 26506

Introduction

Carefully designed experiments, allied with thermochemical kinetics analysis (1) of reaction mechanisms have led to useful working models of complex process such as hydrocarbon pyrolysis, atmospheric chemistry and combustion. A comparable understanding of even the basic chemical features of coal conversion has not yet been developed. Using a combined experimental and thermochemical kinetics approach, this work is intended to lead to effective, semiquantitative chemical models for aspects of coal pyrolysis, polymerization, hydrogenation and liquefaction.

The theoretical foundation for this research is the well-developed understanding (2) and predictive tools (1) for free radical kinetics and thermochemical estimation methods for aromatic substances (3, 4) and free radicals (5). Experiments determine rates of product evolution over as wide a range of conditions as possible with the aim of quantitative description using elementary kinetics models.

Numerous useful experiments using "model" compounds to simulate coal conversion reactions have been reported (6). The present program is not intended to simulate coal reactions, but to reveal characteristic reaction pathways in thermal aromatic chemistry and their kinetic properties, with the aim to eventually extrapolate the results to coal reactions. Two aspects of this program are reported here along with some speculations on coal chemistry.

Experimental

All liquid-phase reactions were carried out in a sealed, evacuated pyrex tube heated in an aluminum block oven. Temperature stability and accuracy were $\pm$ 1°C. Heat-up and cool-down times were generally negligible (< 2 min) relative to reaction duration (15 min - 48 hours). Solids were purified by recrystallization and sublimation and generally found to be 99.5+% pure by gas chromatography (gc). Tetralin was purified by distillation in a spinning band column. GC was the primary analytical tool with benzene and acetone used as solvents for reaction mixtures. Hydrogen, methane and benzene were determined via mass spectrometry. Indentities of products with retention times up to that of phenanthrene were determined by coinjection on a WCOT SE-30 glass capillary column. Other products were determined on OV-101 and FFAP glass columns using temperature programming. Most kinetic analyses were carried out on packed OV-101 glass columns. A more complete account of these experiments is under preparation. The gas phase decomposition rate of 1,2 diphenylethane (12DPE) was determined using very low pressure pyrolysis methods (7).
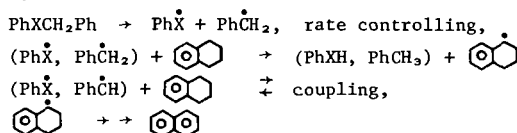
Homolytic Bond Cleavage (R-R' → R• + R'•)

Simple cleavage of covalent bonds to generate two free radicals is commonly regarded as a major first step in coal liquefaction and pyrolysis. Therefore, it is clearly useful to be able to reliably estimate rates of bond cleavage for bonds likely to be present in coal conversion. It is possible at present to estimate rates of such cleavage in the gas-phase for a wide variety of chemical bonds using available thermodynamic and kinetic data (1, 8). While it is commonly assumed that such rate constants are roughly the same in condensed phases as in the gas-phase, this assumption has been well tested only for peroxide decomposition at $\lesssim$ 200° (9).

To directly test the accuracy of the above assumption, rate constants, k_ℓ, of bond scission for 12DPE, benzyl phenyl ether, benzyl phenyl amine and benzyl phenyl sulfide were determined in tetralin solution and compared to corresponding gas phase rate constants, k_g. As shown in Table I, the reliability of this assumption is good.

Gas phase rate constants were determined in the following manner. Very-low pressure pyrolysis was employed to find $k_g(12DPE)/s^1 = 2.9$ at 650°C. By assuming a central C-C bond strength of 61 kcal/mol in 12DPE (10), $\log k_g$ (12 DPE)$/s^{-1} = 14.9 - 61000/4.58$ T. For the remaining substances, k_g was estimated relative to k_g (12DPE) using literature data for related compounds (11).

Liquid phase rate constants were determined in tetralin with the mole fraction of tetralin between 0.8 and 0.95. The dissociation of 12DPE was extensively studied from 325-425°C (Figure 1), and k_ℓ (12DPE)$/s^{-1} = 16-64800/4.58$ T. The mechanism of these reactions was consistent with the following ($X = CH_2$, O, NH, S):

$$PhXCH_2Ph \rightarrow Ph\overset{\bullet}{X} + Ph\overset{\bullet}{C}H_2, \quad \text{rate controlling,}$$

$$(Ph\overset{\bullet}{X}, Ph\overset{\bullet}{C}H_2) + \text{[ring]} \rightarrow (PhXH, PhCH_3) + \text{[ring]}$$

$$(Ph\overset{\bullet}{X}, Ph\overset{\bullet}{C}H) + \text{[ring]} \rightleftharpoons \text{coupling,}$$

$$\text{[ring]} \rightarrow \rightarrow \text{[ring]}$$

In support of this mechanism, the disappearance of $PhXCH_2Ph$ was first order with respect to time and independent of the initial concentration of $PhXCH_2Ph$. The coupling pathway was generally minor, and decreased with increasing temperature. 1,2 Dihydronaphthalene was always seen as a reaction intermediate, while 1,4-dihydronaphthalene could not be detected.

Rate constants, k, (or half-lives, $\tau_{\frac{1}{2}} = \ln2/k$) for a wide variety of bond structural types can now be estimated with reasonable accuracy, and some selected examples are given in Table 3. Of special note is the prediction that under conditions where coal begins to decompose (~ 400°C) the only bonds to appreciably cleave are those that generate two resonance stabilized radicals.

1,2 Diphenylethane Pyrolysis

To develop an understanding of the chemistry of complex systems, it is first necessary to understand the chemistry of "simple" systems as completely and unambiguously as possible. The pyrolysis of 12DPE was chosen as a starting point for these studies since, on paper, it appeared to have a straightforward decomposition pathway, and several relevant rate constants have been measured in solution (2). A complete product analysis has been carried out at 25° intervals over the temperature range 325-450°C. Results at 375°C for the selected products are given in Figure 2. Through analysis via thermochemical kinetics techniques and computer models the mechanism given in Figure 3 has been deduced. Some noteworthy features are:

(1) All features of the reaction can be reasonably interpretated by a free radical scheme.

(2) Combination of 12DPE radicals (step 3a) is favored by $\gtrsim$ 3 over disproportionation (step 3b). This is similar to the behavior of the related 1-phenylethyl radical (2).

(3) A major pathway for trans-1,2-diphenylethene (t-stilbene) production is via radical coupling (step 3a) followed by an H atom abstraction (step 4).

(4) 1,1 diphenylethane results from an uphill ($\Delta G \sim 11$ kcal/mol) "neophyl" rearrangement (2) followed by an H-atom abstraction from 12DPE.

(5) The formation of phenanthrene is hypothesized to occur through an unusual isomerization involving several H-atom shifts.

A set of rate constants consistent with literature values and thermochemical kinetics constraints have been deduced for this mechanism and has been found to adequately predict primary product formation rates up to ~60% decomposition. A

good mass balance has been achieved, and little effect on product formation upon increasing surface area has been found.

Implications for Coal Chemistry

Based on experimental evidence in non-coal systems, and free radical thermo-chemical kinetics, certain specific features of coal conversion chemistry may be suggested.

(1) The first covalent bonds to homolytically cleave upon heating coal are those that generate two resonance stabilized radicals (e.g., benzyl radicals, [structure] ↔ [structure] ↔ ...). In fact, under normal liquefaction conditions (≲ 450°C) such bonds will be virtually the only bonds to break in this manner. Other reaction pathways may generate more reactive organic free radicals, however, these can be expected to abstract benzylic H-atoms, thereby producing resonance stabilized radicals. Hence, to a large extent, the free radical chemistry of coal is determined by the chemistry of resonance stabilized radicals.

(2) Modes of bond rupture other than simple bond cleavage may be very significant in coal reaction. Two well known free radical pathways, β-bond scission,

$$PhCCCPh \xrightarrow{R\cdot} Ph\dot{C}CCPh \rightarrow PhC=C + \cdot CPh \qquad (2)$$
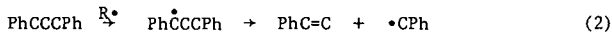
and free radical displacement

$$H\cdot + \overset{R}{\wedge} \rightarrow \overset{H}{\wedge}\overset{R}{\cdot} \rightarrow \overset{H}{\wedge} + R\cdot \qquad (3)$$
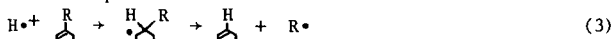
occur in 12DPE (and many other) pyrolyses. The thermal instability reported for the compounds PhCCCPh, PhCCCCPh, PhCOCC in tetralin (6b) are likely due to chain reactions involving sequence (2).

(3) In view of the relatively high temperatures and free radical concentrations (12) in coal conversion, it might be surmised that free radical isomerizations take place under coal conversion conditions which are not observed in conventional solution phase free radical experiments. In fact, the mechanism of Figure 3 contains two such reactions of the 12DPE radical in steps 5 and 6. Isomerization of tetralin and related structures has been reported by several workers A likely path, for instance, for tetralin isomerization to 1-methyl indane (6f) is through the tetralyl radical:

[structures] ⇄ [structure] ⇄ [structure] $\xrightarrow{RH}$ [structure]
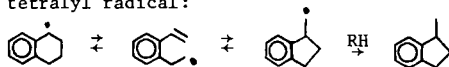
Similar isomerizations can lead to structures which are thermally labile. For instance, a decomposition route for a substituted tetralin structure in coal might be [structure]$_R$ ⇄ [structure]$_R$ ⇄ [structure] $\rightarrow$ [structure] + R·
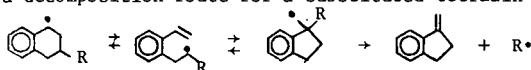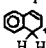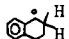
Hence, hydroaromatic structures in coal not only act as H-donors, but may also lead to radical induced bond cleavage.

(4) The unique ability of tetralin and related compounds to act as effective donor solvents cannot be explained simply by its rate of reaction with free radicals (6d). Two other factors concerning high temperature, free radical reactions of tetralin may help explain its special solvent properties.

First, to irreversibly transfer H-atoms to radicals, the donor solvent must be transformed to a substance stable under coal conversion conditions. For instance, diphenyl methane and methyl naphthalene are effective low temperature free radical traps, however, at elevated temperatures the radicals formed upon loss of H-atoms from these molecules cannot be permanently terminated. These radicals will rapidly build up in concentration and act as H-atom acceptors from coal molecules. In support of this idea, we have found that 5:1 mixtures of diphenyl methane:12DPE at 400°C react virtually the same as does pure 12DPE at

this temperature. Despite the fact that PhĊPh radicals are undoubtably the predominant radicals in this system, these radicals will simply build up in concentration, and abstract H-atoms from 12DPE. Substances such as ethyl naphthalene and indane are also not expected to be as effective as tetralin, since their dehydrogenated molecules contain reactive syrene-like structures which may be either reduced by coal back to the starting substance, or aid in the polymerization of coal.

A second, rather unique property of tetralin-like structure is the possible reactive intermediate ⬡⬡ , in which the weak C-H bond strength is only

26 kcal/mol (5). By comparison the weakest C-H bond in ⬡⬡ is 48 kcal/mol.

This radical will lose an H-atom which can be quite effective in depolymerizing coal therough displacement reactions (e.g., 8b in Figure 3).

Conclusion

For the liquid-phase thermal decompositions studied, free radical pathways appear capable of explaining even the finest details in at least a semiquantitative manner.

In our opinion, there is no convincing evidence indicating that homogeneous coal reactions are not primarily free radical in nature. In any case, further complete studies of coal-related pyrolytic systems will indicate not only likely modes of coal reaction via free radical kinetics, but will also reveal contributions from ionic, molecular or heterogeneous pathways.

Acknowledgement
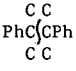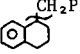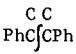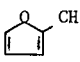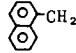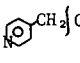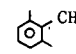
References

1. S. W. Benson, "Thermochemical Kinetics, Second Edition", Wiley and Sons, New York, 1975.
2. "Free Radicals, Vols. I, II", J. Kochi, ed., Wiley and Sons, New York, 1973.
3. S. E. Stein, D. M. Golden and S. W. Benson, J. Phys. Chem., 81, 314 (1977).
4. R. Shaw, D. M. Golden and S. W. Benson, J. Phys. Chem., 81, 1716 (1977).
5. S. E. Stein and D. M. Golden, J. Org. Chem., 42, 839 (1977).
6. (a) C. J. Collins, V. F. Raaen, B. M. Benjamin and G. W. Kabaika, Fuel, 56, 107 (1977); (b) B. M. Benjamin et al., ibid., 57, 269 (1978); (c) Y. Kamilya, T. Yao, S. O. Kawa, Preprints Amer. Chem. Soc. Div. Fuel. Chem., 24 (2), 116 (1979); (d) D. S. Ross and J. E. Blessing, ibid., p. 125; (e) L. W. Vernon, ibid., p. 413; (f) P. S. Virk, et al., ibid., p. 144.
7. D. M. Golden, G. N. Spokes and S. W. Benson, Angew. Chemie, Int. Ed. Engl., 12, 534 (1973).
8. See, for example, J. A. Kerr and A. F. Trotman – Dickinson, "Strengths of Chemical Bonds" in CRC Handbook of Chemistry and Physics, Chemical Rubber Co., Cleveland, OH, 1977.
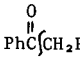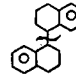9. "Organic Peroxides", D. Swern, ed., Wiley Interscience, New York, 1970.
10. M. Rossi and D. M. Golden, J. Amer. Chem. Soc., 101, 1230 (1979).
11. A. J. Colussi and S. W. Benson, Int. J. Chem. Kinetics, 10, 1139 (1978); 9, 295 (1977); A. J. Colussi, F. Zabel and S. W. Benson, ibid., 9, 161 (1977).
12. L. Petrakis and D. W. Grandy, Analytical Chem., 50, 303 (1978).

Table I. Comparison of Dissociation Rate Constants in Gas-Phase and Liquid (tetralin)-Phase

	$\log k_g$ (est'd)/s^{-1}	k_ℓ (exper)/s^{-1} at T	k_ℓ/k_g at T
PHCH$_2$CH$_2$Ph	15.08-61000/4.58 T	1.02×10^{-5} at 400°C	0.54
PhOCH$_2$Ph	15.58-52800/4.58 T	3.0×10^{-5} at 300°C	1.08
PhNHCH$_2$Ph	15.28-57600/4.58 T	4.4×10^{-5} at 375°C	0.61
PhSCH$_2$Ph	15.58-52700/4.58 T	1.04×10^{-5} at 300°C	0.34

Table II. Liquid Phase Bond Dissociation Rate Constants, k_ℓ, and Half-Lives $\tau_{\frac{1}{2}}$ (θ = 4.58 T/1000)

	$\log k_\ell/s^{-1}$ [a]	$\tau_{\frac{1}{2}}$ (400°C)		$\log k_\ell/s^{-1}$	$\tau_{\frac{1}{2}}$ (400°C)
PhC(CC)(CC)CPh	16.7-54.2/θ [b]	5 sec	(tetralin-CH$_2$Ph)	16.4-61.3/θ [d]	37 min
PhC(CC)CPh	16.3-60.6/θ [b]	20 min	PhO(CH$_2$Ph	16.4-55.0/θ [b]	20 sec
PhCH$_2$(CH$_2$Ph	16.0-64.8/θ [c]	21 hr	(furan-O-CH$_2$(CH$_2$Ph)	16.0-63.3/θ [d]	69 hr
(bicyclic)-CH$_2$(CH$_2$Ph	16.0-62.2/θ [b]	3 hr	PhC(=O)(CH$_2$Ph	16.0-70.8/θ [b]	78 days
(naphthalene-O structure)	16.8-57.6/θ [d]	1 min	(N-heterocycle-CH$_2$(CH$_2$Ph)	16.0-65.8/θ [d]	44 hr
(methyl-substituted-CH$_2$(CH$_2$Ph)	16.0-60.8/θ [d]	1 hr			

[a] Upon substitution of an alkyl group for Ph, k is reduced by ~10^3 at 400° and ~370 at 500°C; $k = Ae^{-E/RT}$, A is accurate to factor of 10, E is accurate ± 5 kcal/mol, k is accurate to factor of 5 (errors in A and E are correlated).

[b] Derived from gas-phase data from literature (see text).

[c] Derived from Figure 1. All other k values are derived from this value by correcting for differences in E and A (reference 1).

[d] Derived from gas-phase data determined in our lab.
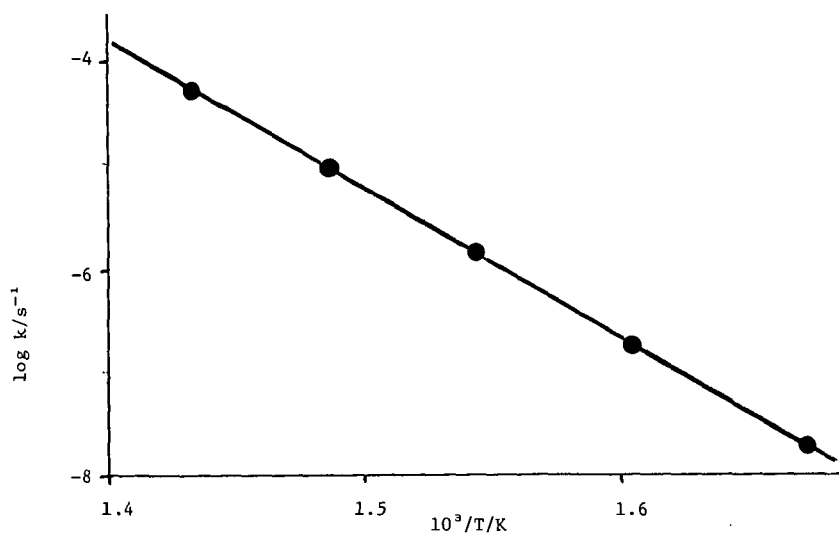
Figure 1. Arrhenius plot for 1,2 diphenylethane dissociation in tetralin
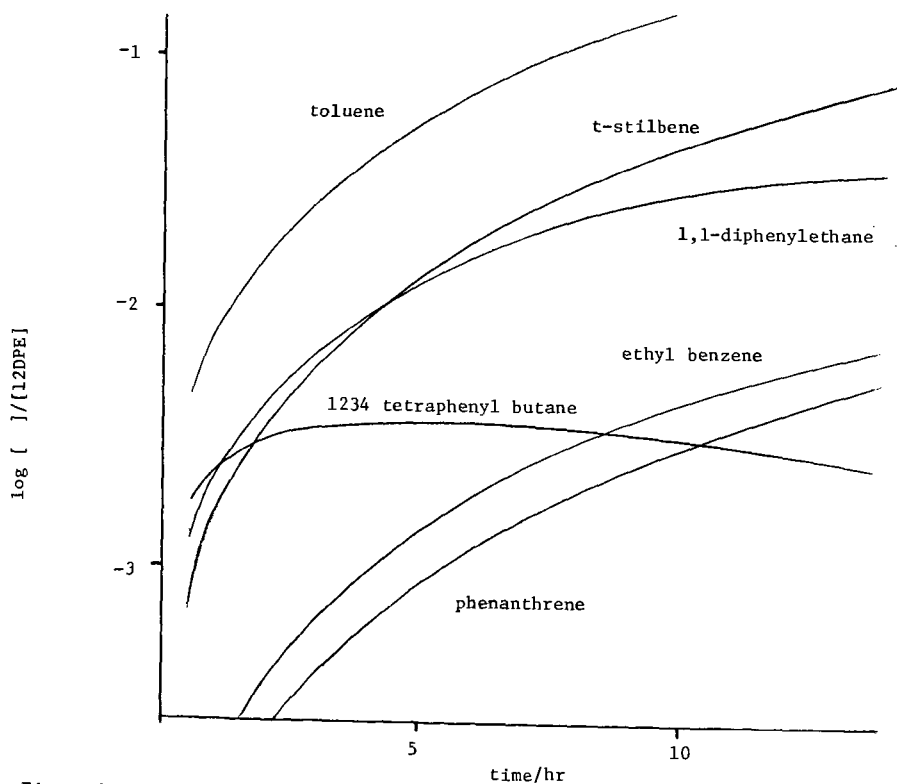
Figure 2. Product evolution in 1,2 diphenyl ethane pyrolysis at 375°C.

Figure 3. Mechanism of 1,2 diphenylethane (Ph = phenyl, R• = PhĊHCH₂Ph) Pyrolysis
(Observed Products are Underlined.)

<u>Major Pathways</u>

(1) PhCH₂CH₂Ph → 2PhĊH₂

(2) PhĊH₂ + PhCH₂CH₂Ph → <u>PhCH₃</u> + PhĊHCH₂Ph

(3) 2PhĊHCH₂Ph

PhCHCH₂Ph
| ⇄ a
PhCHCH₂Ph

         ⇄ b
<u>PhCH=CHPh</u> + PhCH₂CH₂Ph

(4)
PhCHCH₂Ph
| + R• →
PhCHCH₂Ph

PhCHĊHPh
| → <u>PhCH=CHPh</u> + PhĊHCH₂Ph
PhCHCH₂Ph

(5) PhĊHCH₂ ⇄ a / −a

          •
     ⟨Ph   Ph⟩   →b / RH

     ⟨<u>Ph   Ph</u>⟩

<u>Minor Pathways</u>

(6) PhĊHCH₂Ph ⇄ a

→ b / −H

→ R•

(7) PhĊHCH₂Ph → <u>PhCH=CHPh</u> + H

(8) H + PhCH₂CH₂Ph

→ a   <u>H₂</u> + PhĊHCH₂Ph

→ b   <u>PhH</u> + PhCH₂ĊH₂ →RH <u>PhCH₂CH₃</u>

(9) PhĊH₂ + PhĊHCH₂Ph →

PhCH
|
<u>PhCHCH₂Ph</u>

277
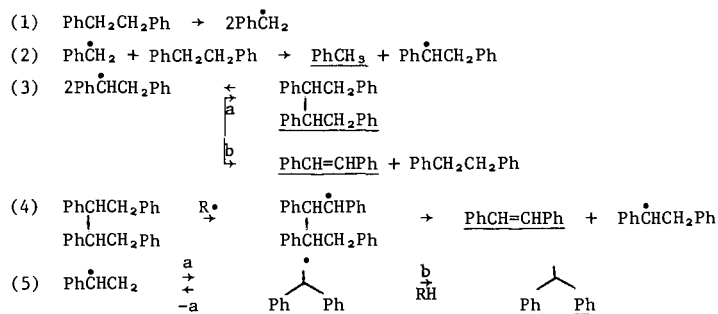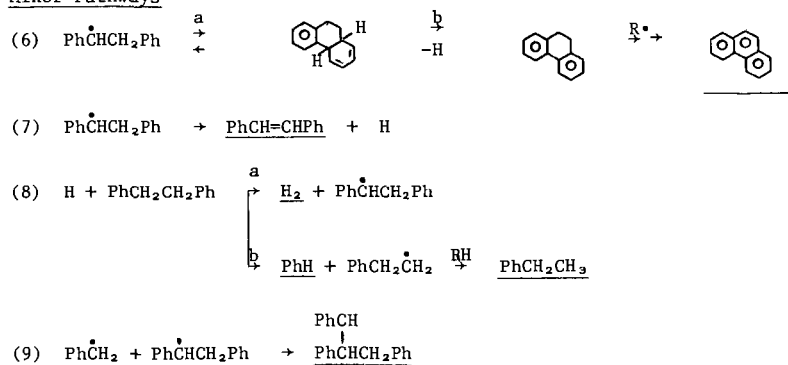
POLYMERIZATION OF PHENANTHRENE INDUCED BY 1-METHYLNAPHTHALENE AT HIGH TEMPERATURES
AND PRESSURES. Curtis L. Knudson, Bruce W. Farnum and Eugene A. Kline. Grand Forks
Energy Technology Center, US DOE, Box 8213 University Station, Grand Forks, ND 58202.

A study of the effects of tetralin and synthesis gas ($CO-H_2$) on the polymerization
of phenanthrene induced by thermally cracked 1-methylnaphthalene at 4000 psi between
440° and 500° C was carried out. Five sets of reactants were studied: (a) phenanthrene
and N_2, (b) 1-methylnaphthalene and N_2, (c) phenanthrene, 1-methylnaphthalene and N_2,
(d) tetralin, phenanthrene, 1-methylnaphthalene and N_2, and (e) phenanthrene, 1-methyl-
naphthalene and $CO-H_2$. The reactants were charged into a cold autoclave, heated to
450° C, and held one hour at each 10° temperature increment up to 500° C. Reactor gas
and liquid phases were sampled during the reactions. Gas samples were analyzed by on-
line GC, and liquid samples were analyzed by gel permeation HPLC, LVMS and GC-MS to
determine composition changes. Results indicated that $CO-H_2$ or tetralin present in the
reactor greatly reduced the polymerization of phenanthrene. Thermal cracking of 1-meth-
ylnaphthalene resulted in alkylation of phenanthrene in preference to 1-methylnaphtha-
lene. Formation of biphenanthryl in preference to 1,2-dinaphthylethane or binaphthyl
occurred in the mixed reactions. Synthesis of the various dimers was carried out to
provide pure reference standards.

REGENERATION OF "SPENT" $ZnCl_2$ PRODUCT CATALYST
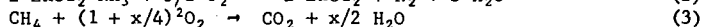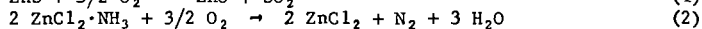FROM HYDROCRACKING SUBBITUMINOUS COAL

Clyde W. Zielke, William A. Rosenhoover and
Robert T. Struck

Conoco Coal Development Company
Research Division
Library, Pennsylvania 15129

INTRODUCTION

It has been demonstrated in batch and continuous bench-scale units that molten zinc chloride is a superior catalyst for liquefaction of coal, coal extract or other heavy hydrocarbons. High quality gasoline of 90-92 Research Octane Number is produced in high yield in a single hydrocracking step (1,2,3,4,5). Large amounts of zinc chloride are used as the catalyst for high activity, i.e., usually 1 gm of $ZnCl_2$ per gm of coal or extract feed. From 1 to 2 parts by weight of product catalyst is generated during the hydrocracking process depending on the $ZnCl_2$/feed ratio. This product catalyst is contaminated with zinc sulfide, ammonia or ammonium chloride complexed with zinc chloride (formed by the catalyst partially reacting with the sulfur and nitrogen in the feed during the hydrocracking step), carbonaceous residue that cannot be distilled out of the melt, and coal ash, when coal is the feed to the hydrocracking process. To keep the catalyst active, these impurities must be removed in a regeneration process in which the catalyst is converted back to essentially pure zinc chloride. The impurities do not settle out of the molten product catalyst; hence, the whole product catalyst must be subjected to the regeneration process. Thus, regeneration is a key step in the $ZnCl_2$ coal liquefaction process in development at Conoco Coal Development Company.

The regeneration is accomplished by burning out the impurities in a combustor containing a fluidized bed of "inert" silica sand:

$$ZnS + 3/2 \ O_2 \ \rightarrow \ ZnO + SO_2 \tag{1}$$
$$2 \ ZnCl_2 \cdot NH_3 + 3/2 \ O_2 \ \rightarrow \ 2 \ ZnCl_2 + N_2 + 3 \ H_2O \tag{2}$$
$$CH_4 + (1 + x/4)^2 O_2 \ \rightarrow \ CO_2 + x/2 \ H_2O \tag{3}$$

Hydrogen chloride gas is added to the feed air to convert ZnO to $ZnCl_2$ and to prevent formation of ZnO by hydrolysis of zinc chloride in the combustor:

$$ZnCl_2 + H_2O = ZnO + 2 \ HCl \qquad K_{927°C} \ = \ \frac{P_{HCl}^2}{(P_{ZnCl_2})(P_{H_2O})} \ \cong 0.24 \tag{4}$$
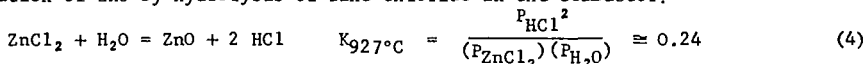
A previous paper described regeneration of essentially coal-ash-free spent melt produced by hydrocracking coal extract (6,7). However, there appear to be economic advantages to a process employing direct coal hydrocracking over a two-step process consisting of coal extraction followed by hydrocracking of the SRC therefrom. Therefore, demonstration of regeneration with low zinc losses of the ash-contaminated spent melt produced by direct hydrocracking of coal is of high importance in the process development. The first work in this regard was done using synthetic spent melt which simulated that produced by hydrocracking subbituminous coal. This work has been published previously (5). Simulated spent melt was used because natural spent melt was not available. Subsequent to that work, successful direct hydrocracking with $ZnCl_2$ catalyst of Colstrip subbituminous coal in a continuous bench-scale hydrocracker furnished feedstock for further development of the regeneration process. Continuous regeneration of this coal-ash-contaminated spent melt from direct hydrocracking of coal and efficient zinc recovery therefrom has now been demonstrated for the first time. In this work zinc recovery was enhanced by introducing a secondary zinc recovery step in which zinc, retained in the coal ash rejected in the primary regeneration step, is largely recovered. This paper presents some of the results of this regeneration work with natural spent melt from direct coal hydrocracking.

EXPERIMENTAL

Feedstocks

Spent Melt

The two feedstocks for the primary regeneration work were low-carbon spent melts produced by direct hydrocracking of Colstrip coal in a 3 lb/h continuous bench-scale hydrocracking unit. Hydrocracking conditions were: 413°C, 24.13 MPa (3500 psig), $ZnCl_2$/MF solvent-free Colstrip coal ratio of 1.5 and residence times ranging from 74 to 95 min. Normally a $ZnCl_2$/coal ratio of 1.0 is used; the higher ratio of 1.5 was used to speed up production of spent melt. It gave a yield of about 1.75 gm of spent melt per gm of MF coal feed vs. about 1.25 which is produced at a $ZnCl_2$/coal ratio of 1.0. The carbon content of the two spent melt feedstocks used were 6.65 and 6.31%, slightly more than required to furnish the heat when burned for carrying out the regeneration adiabatically. The total ash content of the feed melt is based on the sum of the eight most prevalent coal ash elements (Na, K, Ca, Mg, Fe, Ti, Si, Al) expressed as oxides, since the coal ash is mixed with non-combustible materials and, therefore, cannot be determined directly. The total ash determined in this manner is. lower than the ash determined in coals or chars in the conventional manner, where sulfates and carbonates may be present, that are not taken into account here. Also, traces of minor elements are not considered here. Analyses of the spent melt are given in Table I.

Colstrip Coal

Minus 100 mesh Colstrip subbituminous coal (Rosebud Seam, Montana) was used as the feedstock for testing, in a 3 lb/h continuous hydrocracker. The activity of regenerated spent melt was compared with virgin zinc chloride. Analyses of this coal are given in Table I.

Cyclone Underflow Ash

This material, which is generated in the primary regeneration step, contains the coal ash and generally less than 2% of the zinc in the spent melt feed to the primary regeneration. It is fed to a secondary zinc recovery step wherein the majority of this "lost" zinc is recovered. Analyses of this material are given under the heading "Composite" in Table VI.

Equipment and Procedure

Primary Regeneration

Figure 1 is a diagram of the continuous 2-7/8" I.D. fluidized bed combustion unit in the configuration used for primary regeneration. The molten "spent" catalyst is fed via a Fluid Metering, Inc. Lab Pump and is dropped from a remote drip tip into a batch bed of fluidized silica sand. The feed gas consists of a mixture of air and anhydrous hydrogen chloride which enters at the apex of the reactor cone. In the fluidized bed, the zinc chloride is vaporized, the carbon, nitrogen and sulfur impurities are burned out and any zinc oxide is largely converted to zinc chloride by the HCl in the feed gas. The gas and zinc chloride vapor entrain the coal ash, leave the reactor and pass through the cyclone where the solids are collected. The cyclone underflow solids derive solely from the melt since the sizing of the silica sand bed solids is such that there is essentially no elutriation of this material. The solids collected at the cyclone then consist largely of coal ash contaminated by small amounts of zinc in the form of zinc chloride and zinc oxide or other compounds, and any unburned carbon or zinc sulfide. The gas then passes to the condenser where zinc chloride is condensed, then to the electrostatic precipitator to remove zinc chloride fog, and then to sampling and metering. The analytical methods and calculational procedures are substantially the same as those previously described (7).

Hydrocracking

The hydrocracker and its operating procedure have been described previously (9).

Secondary Regeneration

The apparatus used to conduct the secondary recovery studies was the same unit used for the primary regeneration studies with some modifications made to accommodate the use of a solid feed. The modifications consisted of replacing the melt feed system with a metering powder feeder for feeding the cyclone underflow solids to the unit. The drip tip was plugged off since it was not used.

The cyclone underflow ash is fed at a metered rate into the air feed gas line that transports the ash into the bottom of the batch fluidized bed of silica sand. Anhydrous HCl is injected into the air stream just upstream from the reactor. Some of the ash is temporarily trapped in the fluidized bed of silica sand, building up to a steady-state concentration. The remainder of the ash is carried out of the bed by the gas stream. At steady state, the amount of ash fed per minute equals the amount of ash per minute that is transported by the gas stream out of the bed. The average ash residence time in the reactor in minutes is then "grams of ash inventory in the bed divided by the ash feed rate in grams per minute."

The gas, $ZnCl_2$ vapors, and entrained ash leave the reactor and follow the same course described above for primary regeneration.

The feed gas is electrically preheated to 316°C (600°F) before it enters the reactor. The remaining heat required is put in through the reactor walls by electrical heaters.

The run was started when the cyclone underflow ash feed to the reactor started. The product cyclone underflow was collected in 5 to 10 min. increments as a function of running time. The run was ended when the ash feed stopped.

The ash inventory in the bed was measured to enable precise calculation of the average residence time in the bed.

Run duration was about 40 minutes, which required about 200 grams of ash per run. This was low enough that the relatively limited ash supply was sufficient to conduct a reasonably complete program. Thus, in runs of 10-12 minutes residence time, the longest times investigated, there were at least three changes of ash inventory.

The reaction was followed by analyzing the product ash increments for total and water-soluble zinc, chlorine and iron. Steady state was indicated by constant concentrations of zinc in the increments.

In general, complete material and elemental balances were not made because the small amount of material collected in the labyrinthine collection equipment downstream from the cyclone made accurate collection of small amounts of product very difficult. Instead the yield of effluent ash was determined by a silica balance around the ash in and the ash out. This, together with metals analyses of the feed and product ash, provided the data for calculation of metals removal.

RESULTS AND DISCUSSION

Primary Regeneration

The variables and the levels at which they were investigated are:

Temperature, °C	871, 927, 954, 982
Pressure, kPa (psig)	119 (3)
% of Stoichiometric Air (nominal)	115
Mol % of Anhydrous HCl in Feed Air	5.5, 8.5, 11.5
Fluidized Bed Solids	297 x 595 μm Silica Sand
Fluidized Bed Depth, meters	0.305
Superficial Linear Velocity, meters/sec	0.305

Operability

The criterion for operability is that the coal ash leaves the bed by elutriation and that it is not retained in the bed due to size growth by sintering or clinker formation. Based on this criterion operability was as follows:

1. With 5.5% HCl in the inlet air:

    a. 927°C (1700°F) is an operable condition, at least for short period.
    b. 954°C (1750°F) is a marginally operable condition because of some sintering of ash in the bed.
    c. 982°C (1800°F) is an inoperable condition because of severe ash sintering in the bed leading to clinker formation.

2. With 8.5 or 11.5% HCl in the inlet air:

    a. 927°C is an operable condition.
    b. 954°C is an operable condition.
    c. 982°C probably is a marginally operable condition with some minor size growth in the ash grain size to be expected. This may be desirable from the standpoint of preventing ash buildup in the regenerated melt.

Some slight sintering may be desirable to give more efficient cyclonic removal of the ash from the gas stream. The sintering that restricts operability is likely promoted by the fluxing action of ash metal chlorides (NaCl, KCl, $CaCl_2$, $MgCl_2$) that can be formed in the hydrocracker by reactions such as

$$Na_2O + ZnCl_2 = 2 \ NaCl + ZnO$$
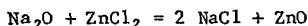
In general, 927°C was found to be the preferred temperature in that the temperature was low enough for good operability but high enough for good reaction kinetics, yielding efficient burnout of the impurities.

Results

The results presented will be confined to work done at 927°C and the effect of HCl concentration in the air on these results. Table II shows conditions and material balances for runs at 927°C with 5.5, 8.5 and 11.5 mol % HCl in the feed gas. Table II shows that good material balances were obtained. Products derived from four sources: the product melt, cyclone underflow solids, bed solids, and gas which includes water. The bed solids yield per unit of feed decreases as run duration, and hence the total amount of melt fed, increases, since a batch bed of silica was used.

Table III shows the efficiency of regeneration for the three runs whose material balances have been given. Zinc recovery with 5.5% HCl in the feed air was 97.9% and it increased to 99.1% with 11.5% HCl in the feed air. Higher recovery is achieved with higher HCl concentration because the $ZnCl_2$ hydrolysis equilibrium is shifted farther to the $ZnCl_2$ side.

Recoveries of chlorine (Table III) greater than 100% of the chlorine in the feed melt reflect conversion of ZnO and ZnS in the feed to $ZnCl_2$ by interaction with the HCl in the gas.

The small amounts of nitrogen, carbon and sulfur in the product melts (Table III) reflect the high efficiency of burnout of the NH_3, ZnS and carbonaceous residue, since essentially all of the remaining carbon, nitrogen and sulfur are in the unit offgases as combustion products: SO_2, CO, CO_2, N_2 and H_2O. Nitrogen and sulfur burnout were generally greater than 97% and carbon burnout was greater than 99%.

The low percentage of the feed ash in the product melt (Table III) shows that ash rejection at the cyclone was very efficient. Rejection of the individual metals of which the ash is comprised, was also efficient except for sodium and potassium, most of which appear in the melt. This is undoubtedly due to the formation of the highly-stable NaCl and KCl which are slightly volatile at regeneration

conditions (~ 3 and 5 torr vapor pressure at 927°C, respectively). A substantial fraction of the iron, most likely as $FeCl_2$ also appears in the melt. Over many cycles of hydrocracking and regeneration, vapor-liquid equilibria with respect to NaCl and KCl at a regeneration temperature of 927°C will limit the buildup of the sum of their concentrations in the $ZnCl_2$ catalyst to about 1.0 to 1.5 mol % when the regeneration is conducted at 3 atm pressure or even less at higher pressures. The hydrolysis equilibrium

$$FeO_{(s)} + 2\ HCl_{(g)} = FeCl_{2(g)} + H_2O_g \qquad K_{927°C} = \frac{P_{FeCl_2}P_{H_2O}}{P_{HCl}^2} \cong 0.24 \qquad (5)$$

or reactions such as

$$FeCl_2 + H_2O + ash = FeO \cdot ash + 2\ HCl$$
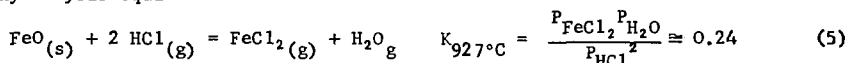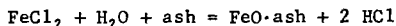
will restrict the $FeCl_2$ concentration in the regenerated $ZnCl_2$ catalyst to less than 10 mol %. A run in which the melt to regeneration was spiked with $FeCl_2$ tends to confirm this. Batch hydrocracking data indicate that, at these levels, these ash metal chlorides present essentially no problem regarding catalyst activity.

Table IV shows analyses of the product regenerated melts. The melts obviously are close to pure $ZnCl_2$ since the Zn:Cl atomic ratios are 1.95, 1.97 and 2.02.

After separating out the trapped ash and sampling, the used 28 x 48 mesh silica sand bed solids were employed in consecutive runs. The silica bed is almost inert to interaction with zinc and chlorine as shown by their extremely small contents in the silica sand bed after 54 hours of use in spent melt regeneration (Table V). There is some reaction of calcium and magnesium with the silica sand bed as indicated by an increase with time up to the concentrations of 1.49 and 0.44% of CaO and MgO after 54 hours.

Table VI gives analyses of the coal ash rejected by the cyclone during primary regeneration. The yields of these ashes were about 5.8% per 100 grams of feed melt exclusive of the steady-state concentration of ash trapped in the bed when the run was terminated. These ashes contain essentially all of the feed zinc not found in the product melt. The zinc retained in the ashes represent 1 to 2% of the feed zinc to regeneration, the retained zinc being lower when the HCl concentration in the air increases. It is in two forms: 1) zinc in the form of zinc chloride (water-soluble zinc) which is adsorbed on, entrained by, or diffuses to the cyclone underflow ash during the regeneration process, and 2) zinc in the form of ZnO, $ZnO \cdot SiO_2$ and $ZnO \cdot Al_2O_3$ (water-insoluble zinc) which is not completely converted to the $ZnCl_2$ because of equilibrium restrictions in reaction (4) and reactions of the type

$$ZnCl_2 + SiO_2 + H_2O = ZnO \cdot SiO_2 + 2\ HCl \qquad (6)$$
$$ZnCl_2 + Al_2O_3 + H_2O = ZnO \cdot Al_2O_3 + 2\ HCl \qquad (7)$$
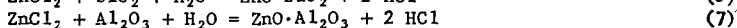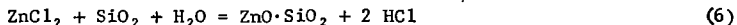
Accordingly, the concentration of the water-insoluble zinc decreases as the HCl concentration in the feed air increases, whereas the water-soluble ash concentration remains more or less constant.

Since 1% zinc "loss" represents about 4¢ per gallon gasoline, recovery of the zinc in the ash is worthwhile from the economic aspect as well as from the environmental and conservation aspects. Therefore, investigations of "Secondary Zinc Recovery," that is, recovery of the zinc retained in the cyclone ash were made.

Secondary Zinc Recovery

Secondary recovery consisted of treatment of the cyclone underflow ash from the primary regeneration with $ZnCl_2$-free air plus HCl. The principle of this treatment is to reverse equilibria such as in reactions (4), (6) and (7) so that the water-insoluble zinc values are converted to $ZnCl_2$ which is evaporated from the ash substrate and recovered.

The cyclone ash used as feed in this work was a composite from a number of primary regeneration runs. Analysis of this feedstock is given in Table VI.

The levels of the variables studied in secondary zinc recovery are tabulated below:

Temperature, °C	816, 927, 1038
°F	1500, 1700, 1900
Pressure, kPa	119, 195, 271
psig	3, 14, 25
Mol % Anhydrous HCl in Feed Air	0 to 60
Feed Ash Residence Time, min	1.5 to 12.7
Fluidized Bed Solids	297 x 595 μm Silica Sand
Fluidized Bed Depth, meters	0.013, 0.062, 0.124
Superficial Linear Velocity, meters/sec	0.18, 0.24, 0.30

Operability

Runs at all conditions tested gave excellent operability. No sintering of ash was found in any of the runs, even those at 1038°C.

Results

Figures 2, 3 and 4 summarize the results.

Figure 2 shows the breakdown of the recovery of water-soluble and water-insoluble zinc as functions of time and temperature, with a feed gas consisting of 20 mol % HCl in air. Essentially 100% of the water-soluble zinc in the cyclone ash was recovered in as little as one minute residence time at all the conditions tested. This is not surprising since no reaction is required, only volatilization of the $ZnCl_2$ that the water-soluble zinc represents. It has been shown that HCl is not required for this H_2O-soluble zinc recovery, that essentially 100% recovery can be obtained using HCl-free air or nitrogen. Figure 2 shows that the extent of secondary recovery of zinc is limited by the rate of reaction of the water-insoluble zinc to form volatile zinc chloride. The rate of recovery of the water-insoluble zinc is very fast initially but slows down markedly after the first minute of reaction time. Recovery is better the higher the temperature in the range of 816 to 1038°C.

Figure 3 is a plot similar to Figure 2 but it shows the total combined recovery of water-soluble and water-insoluble zinc. It is apparent from this plot that as high as 70% of the total zinc in the cyclone solids was recovered in as little as one minute residence time.

Greater than 73% of the chlorine in the cyclone underflow ash was volatilized and removed from the feed ash at all conditions tested.

Figure 4 shows that the water-insoluble zinc recovery increases moderately with increasing HCl partial pressure. The increase is unaffected by the HCl/air ratio. Hence, at a given HCl concentration in the feed air, the zinc recovery can be enhanced by increasing the total pressure and thereby the HCl partial pressure. Therefore, at the projected commercial operating pressure of 5 atm, 4 mol % HCl in the feed air should give results equivalent to the use of 20% HCl at 1 atm.

Thus, it has been shown that 70% or more of the zinc in the ash retained in the cyclone solids can be recovered in a relatively simple step added to the primary regeneration system. With secondary recovery of 70%, overall zinc recovery of 99.6 to 99.7% has been demonstrated. The secondary zinc recovery gives a savings in zinc makeup costs of about 3.5¢ per gallon of gasoline produced from coal via the $ZnCl_2$ process (8).

Hydrocracking Activity of Regenerated Melt

A run was made in the continuous bench-scale 3 lb/h hydrocracker in which the product $ZnCl_2$ catalyst from regeneration Run 19 was tested in hydrocracking Colstrip coal. As shown in Table VII, the regenerated catalyst was somewhat more reactive

than virgin zinc chloride. This is likely due to the fact that the regenerated catalyst contained less ZnO, which depresses $ZnCl_2$ activity, than the virgin zinc chloride.

References

1. Consolidation Coal Co., R&D Report No. 39, Office of Coal Research, U. S. Dept. of the Interior. Interim Report No. 2, "Research on Zinc Chloride Catalyst for Converting Coal to Gasoline--Phase I--Hydrocracking of Coal and Extract with Zinc Chloride," Vol. III, Book 1, March, 1968.

2. Zielke, C.W., Struck, R.T., Evans, J.M., Costanza, C.P., Gorin, E., "Process Design Develop.," Ind. Eng. Chem. (1966) 5, 151.

3. Ibid., 158.

4. Struck, R.T., Clark, W.E., Dudt, P.J., Rosenhoover, W.A., Zielke, C.W., Gorin, E., Ind. Eng. Chem. (1969) 8, 546.

5. Zielke, C.W., Rosenhoover, W.A., Gorin, E. -- Shale Oil, Tar Sands, and Related Fuel Sources (T. F. Yen, ed.) Advances in Chemistry Series No. 151, 153 (1976).

6. Zielke, C.W., Struck, R.T., Gorin, E., Ind. Eng. Chem. (1969) 8, 552.

7. Consolidation Coal Co., R&D Report No. 39, Office of Coal Research, U. S. Dept. of the Interior. Interim Report No. 2, "Pre-Pilot Plant Research on the CSF Process--Phase I--Regeneration of Zinc Chloride Catalyst," Vol. III, Book 2, March 1968.

8. Parker, W.A., et al., Conoco Coal Development Co. Report No. FE-1743-45 to DOE, Nov. 20, 1977.

9. Zielke, C.W., Klunder, E.B., Maskew, J.T. and Struck, R.T., "Continuous Hydro-liquefaction of Subbituminous Coal in Molten Zinc Chloride," presented at the 85th National Meeting, A.I.Ch.E., Philadelphia, Pa., June 1978. Submitted for publication in I&EC, Proc. Des. Dev.

TABLE I

Analysis of Feedstocks for Primary Regeneration and Coal Hydrocracking

	"Spent" ZnCl₂ Melt, Feed to Primary Regeneration		-100 Mesh Colstrip Coal, Feed to Hydro-cracking
	F-6	F-7	
Volatile Matter			41.73
Ash (SO₃-free)	4.82	5.51	12.53
Organic Hydrogen	0.77	0.69	4.03
Carbon	6.65	6.31	66.53
Organic Nitrogen	0.22	0.05	1.00
Oxygen (by diff.)			14.72
Organic Sulfur	0.03	0.00	0.92
Pyritic Sulfur			0.27
Sulfate Sulfur			0.05
ZnCl₂	80.28	77.36	
ZnS	0.91	1.28	
ZnO	2.71	3.31	
NH₃	0.56	0.72	
Unidentified	3.03	4.72	
	Ash Composition, Wt. %		
Na₂O	1.02	0.53	0.31
K₂O	0.40	0.27	0.31
CaO	13.43	13.58	12.72
MgO	5.09	5.36	5.59
Fe₂O₃	9.37	8.93	7.55
TiO₂	1.90	1.48	1.07
SiO₂	49.46	52.34	51.33
Al₂O₃	19.33	17.51	21.45

TABLE II

Primary Regeneration
Conditions and Material Balances

Run Number	16	22	19
Reactor Temperature, °C		927	
% Stoichiometric Air	115	125	119
Pressure, psig		3	
Superficial Linear Velocity, m/sec		0.305	
Fluidized Bed Depth, m		0.305	
Inlet Gas Composition, Mol %			
Air	94.5	91.5	88.5
Anhydrous HCl	5.5	8.5	11.5
Melt Feed Rate, kg/h/m²	305	299	294
Run Time, h	4.0	10.9	22.1
Feedstock Used	F-6	F-7	F-6
In, gm/100 gm Feed Melt			
Feed Melt	100.00	100.00	100.00
Air (ex argon)	126.52	129.16	131.17
Anhydrous HCl	9.39	15.25	21.78
Bed Solids	26.66	10.04	4.99
Total	262.57	254.45	257.94
Out, gm/100 gm Feed Melt			
Product Melt	83.73	85.39	85.57
Cyclone Solids	3.86	5.79	4.92
Bed Solids	28.93	10.62	5.46
HCl	8.80	17.47	22.02
H₂O	7.48	6.30	6.72
CO₂	20.96	22.36	25.78
CO	1.90	1.86	1.60
SO₂	1.01	0.81	0.40
N₂	102.00	96.65	95.04
O₂	6.65	7.15	6.33
Total	266.30	254.37	253.84
(Out/In)(100)	101.4	100.0	98.4

TABLE III

Efficiency of Primary Regeneration

Run No.	16	22	19
Mol % HCl in Air	5.5	8.5	11.5

	% of Feed Melt Component in Regenerated Melt		
Zn	97.9	98.8	99.1
Cl	102.0	107.3	106.2
C	0.6	0.7	0.9
S	9.7	2.0	2.4
N	0.0	2.7	2.5
Total Coal Ash	6.4	3.2	4.4
Na	63	92	75
K	80	122	66
Ca	1.9	1.7	2.6
Mg	1.7	1.4	2.6
Fe	33	12	20
Si	1.6	1.2	1.7
Al	2.1	1.7	0.2

TABLE V

Primary Regeneration Analysis of Effluent Bed Solids

Run No.	19	22
Hours Used	32	54

	Weight %	
H	0.06	0.03
C	0.34	0.06
N	0.00	0.00
S	0.01	0.02
Zn	0.05	0.15
Cl	0.00	0.00
Na_2O	0.02	0.01
K_2O	0.05	0.04
CaO	0.78	1.49
MgO	0.30	0.44
Fe_2O_3	0.20	0.19
TiO_2	0.04	0.00
SiO_2	97.35	96.23
Al_2O_3	0.79	1.30

TABLE IV

Primary Regeneration Analysis of Product Melts

Run No.	16	22	19
Anal. of Melt, Wt. %			
H	0.15	0.13	0.17
C	0.05	0.05	0.07
N	0.00	0.02	0.02
O (by diff.)	1.49	1.63	0.40
Organic S	0.00	0.00	0.00
Sulfide S	0.04	0.01	0.01
Sulfate S	0.00	0.00	0.00
Zn	47.61	47.40	47.32
Cl	50.30	50.59	51.83
Ash	0.36	0.17	0.18
Anal. of Ash, Wt. %			
Na_2O	10.22	19.00	24.98
K_2O	5.23	12.55	8.71
CaO	4.03	9.20	11.29
MgO	1.43	3.01	4.36
Fe_2O_3	49.21	19.55	20.11
TiO_2	11.06	1.73	1.46
SiO_2	12.41	23.68	27.72
Al_2O_3	6.41	11.28	1.37

TABLE VI

Primary Regeneration
Analysis of Cyclone Underflow Solids

Run No.	16	22	19	Composite
% HCl in Feed Air	5.5	8.5	11.5	
Analysis, Wt. %				
Zn in $ZnCl_2$*	4.73	3.57	4.10	2.94
Zn in ZnO, $ZnO \cdot SiO_2$, $ZnO \cdot Al_2O_3$**	11.08	4.07	3.33	4.54
Cl	5.30	4.80	5.54	4.92
H	0.11	0.12	0.13	0.08
C	0.35	0.14	0.35	0.09
S (sulfate)	0.34	0.30	0.23	0.37
Na_2O	0.17	0.08	0.12	0.10
K_2O	0.04	0.02	0.02	0.03
CaO	9.65	11.87	9.48	11.40
MgO	4.04	4.41	4.14	4.45
Fe_2O_3	3.67	4.06	2.98	3.90
TiO_2	0.67	0.00	0.84	0.94
SiO_2	33.36	44.75	43.21	42.86
Al_2O_3	14.20	18.19	19.48	18.41

* Water-soluble zinc
** Water-insoluble zinc

TABLE VII

Comparison of Hydrocracking
Results With New and Regenerated
$ZnCl_2$ Catalyst

Conditions		
Feedstock	-100 Mesh Colstrip Coal	
Temperature, °C	399	
Total Pressure, psig	3500	
Melt Residence Time, h	1.29	
$ZnCl_2$/MF Coal, Wt. Ratio	1.0	

	Regenerated $ZnCl_2$ Catalyst	New $ZnCl_2$ Catalyst
Yields, Wt. % MAF Coal		
C_1-C_3	1.2	2.1
C_4	4.2	2.7
C_5 x 200°C Distillate	41.5	33.5
200 x 475°C Distillate	16.2	20.9
+475°C Distillate	6.0	6.1
MEK-Soluble Residue	17.7	15.8
MEK-Insoluble Residue	2.5	4.9
H Consumed	6.4	6.8
Conversion to Distillate	79.8	79.3

FIGURE 1

SIMPLIFIED FLOW DIAGRAM OF BENCH-SCALE (4 LB/HR) REGENERATOR

To Gas

Metering
and
Scrubbing

Drying
Tower

C.W.

Electro-
static
Precipi-
tator

Moisture
Collection

Demister

to H_2O Condensation
and Recycle

$ZnCl_2$ Cond-
enser

Cooling
H_2O + Air

Cyclone

Coal Ash
Receiver

Coal Ash
Out

Mullite
Liner
2-7/8" ϕ x 24"

Regenerated
Melt
Collection
System

Melt Out

Drip
Tip

Fluidized
Combustor

Anh.
HCl

Air

Frozen
Spent
$ZnCl_2$ Melt

Melt
Tanks

Spent
Melt
Weigh
Tank

Spent
Melt
Pump

SECONDARY ZINC RECOVERY GRAPHS

FIGURE 2

Zinc Type Recovery as a Function of Temperature and Time
Total Pressure = 3 psig; Feed Gas = 20 mol % HCl in Air

FIGURE 3

Total Zinc Recovery as a Function of Temperature and Time
3 psig; 20 mol % HCl in Air
Key is same as for Figure 2

FIGURE 4

Water-Insoluble Zinc Recovery vs. HCl Partial Pressure
Residence Time = 10 min; Temperature = 927°C
Total Pressure of Run is listed at Data Points